Supplementary Information

Expanding Elastic Moduli Bounds in Solid-Void Metamaterials: Poisson's Ratio Dependence and Optimal Design

Cihan Tekoğlu[1,*], Oguz Aycan Ickin[1]

[1] *Department of Mechanical Engineering, TOBB University of Economics and Technology, Söğütözü, Ankara, 06560, Türkiye*

Supplementary Text

A. Upper bounds on the elastic moduli of two-phase solid-void isotropic materials

B. Mechanical properties and mechanisms of infinite periodic trusses trough matrix methods

C. Deformation mechanisms in lattice materials

Supplementary Figs. 1-3

Appendix A: MATLAB code for the structural analysis of the twisted Kagome trusses

Appendix B: MATLAB code for the structural analysis of the hexachiral trusses

Appendix C: MATLAB code for the structural analysis of the double triangular trusses

*Corresponding author. Tel.:+90 312 292 40 65
Email addresses: cihantekoglu@etu.edu.tr; c.tekoglu@gmail.com (Cihan Tekoğlu)

A. Upper bounds on the elastic moduli of two-phase solid-void isotropic materials

In the following, E, G, and K represent Young's modulus, shear modulus, and bulk modulus, respectively, and ν denotes Poisson's ratio. When these parameters are written without subscripts, they refer to the properties of the solid-void composites; when accompanied by the subscript "s", they describe the properties of the solid phase. The subscript "HS" indicates the Hashin-Shtrikman upper bounds [1, 2], "CGD" refers to the upper bounds for beam networks in 3D derived by Christensen [3] and Gurtner and Durand [4], and "NUB" denotes the new upper bounds introduced in this study. Poisson's ratio of the dense solid phase, ν_s, ranges from -1 to 0.5, for both 2D and 3D composites, with the exception of hierarchical lattices (section A.3), wherein the solid phase itself comprises a lattice structure on successively smaller scales, and therefore $-1 < \nu_\mathrm{s} < 1$. Furthermore, $\bar{\rho}$ denotes the relative density of the composite.

A1. 2D materials

When expressed in terms of the relative density $\bar{\rho}$ of the composite and Poisson's ratio ν_s of the solid material, the Hashin-Shtrikman upper bounds in 2D have the following form:

$$\frac{E_\mathrm{HS}}{E_\mathrm{s}} = \frac{\bar{\rho}}{3 - 2\,\bar{\rho}}, \tag{A1}$$

$$\frac{G_\mathrm{HS}}{E_\mathrm{s}} = \frac{\bar{\rho}}{8 - 2\,\bar{\rho}(3 - \nu_\mathrm{s})}, \tag{A2}$$

$$\frac{K_\mathrm{HS}}{E_\mathrm{s}} = \frac{\bar{\rho}}{4 - 2\,\bar{\rho}(1 + \nu_\mathrm{s})}, \tag{A3}$$

$$\nu_\mathrm{HS} = \frac{1 - \bar{\rho}(1 - \nu_\mathrm{s})}{3 - 2\,\bar{\rho}}. \tag{A4}$$

Supplementary Fig. 1a illustrates the evolution of ν_HS (equation A4), which represents the Poisson's ratio of a composite that satisfies the Hashin-Shtrikman (HS) upper bounds for a given combination of $\bar{\rho}$ and ν_s, as a function of ν_s. When $\bar{\rho} = 1$, ν_HS is equivalent to ν_s, as expected. For $\bar{\rho} < 1$, ν_HS is confined within the limits of $\nu_\mathrm{HS\text{-}min}$ and $\nu_\mathrm{HS\text{-}max}$, where $\nu_\mathrm{HS\text{-}min}$ corresponds to $\nu_\mathrm{s} \to -1$ (i.e., $\nu_\mathrm{HS}\,|_{\nu_\mathrm{s}\to -1}$) and $\nu_\mathrm{HS\text{-}max}$ corresponds to $\nu_\mathrm{s} \to 0.5$ (i.e., $\nu_\mathrm{HS}\,|_{\nu_\mathrm{s}\to 0.5}$). As $\bar{\rho}$ decreases, the range of ν_HS progressively narrows.

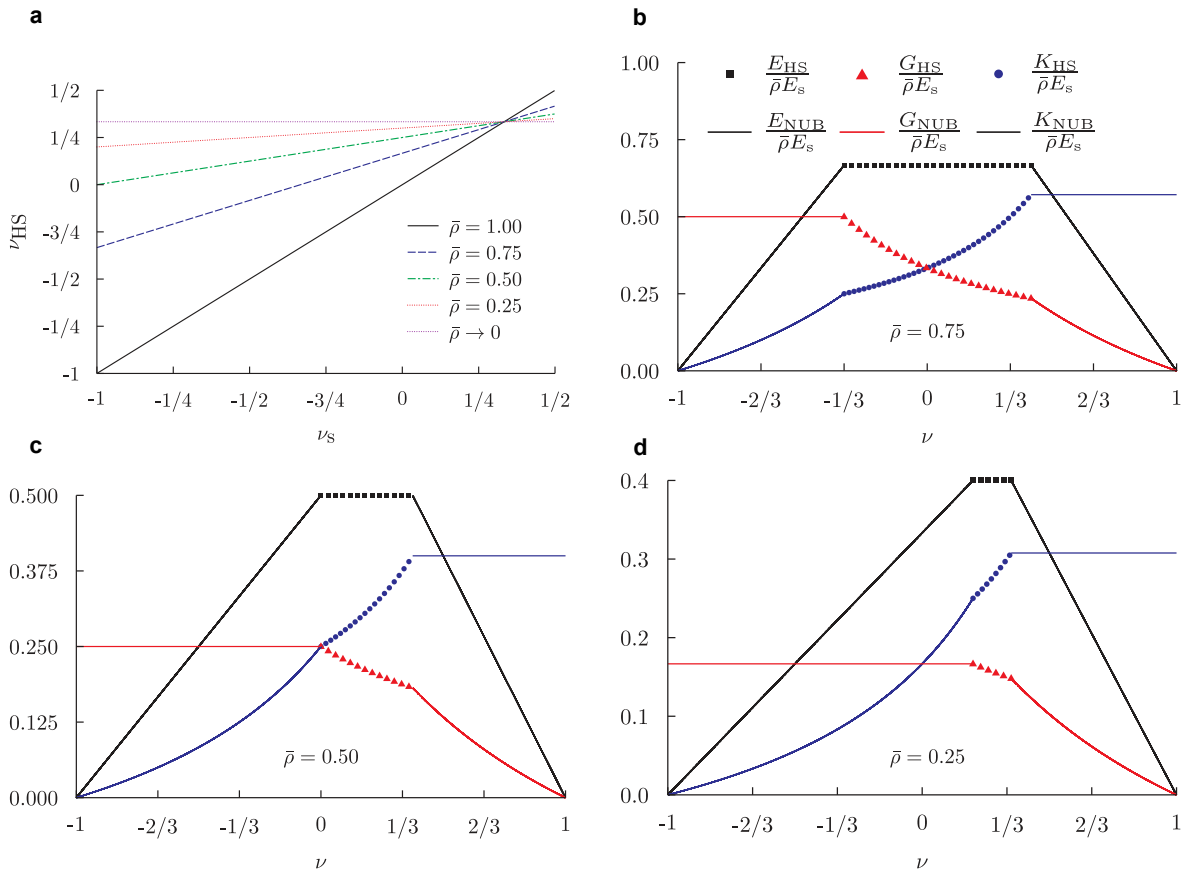

Supplementary Fig. 1 | Upper bounds on the elastic moduli of two-dimensional two-phase solid-void isotropic composites. a, Variation of ν_{HS} (Poisson's ratio of a composite adhering to the HS upper bounds for a specific combination of relative density, $\bar{\rho}$, and solid material Poisson's ratio, ν_s; see equation A4), as a function of ν_s. **b-d,** Evolution of the upper bounds for Young's modulus, shear modulus, and bulk modulus as functions of the composite Poisson's ratio, ν (see equations A5-A14), for $\bar{\rho}$ values of 0.75, 0.50, and 0.25, respectively.

To elucidate the significance of the limits $\nu_{HS\text{-}min}$ and $\nu_{HS\text{-}max}$, consider 2D lattices at the low-density limit ($\bar{\rho} \ll 1$), where ν_{HS} converges to a single value: $\nu_{HS\text{-}min} = \nu_{HS} = \nu_{HS\text{-}max} = 1/3$. For instance, take the infinite periodic Kagome truss, in which all cell walls align with one of the three symmetry lines (labelled I, II, and III in Extended Data Fig. 1a).

When the Kagome truss is subjected to uniaxial loading along one of its symmetry lines, the cell walls aligned with the loading direction deform purely through stretching. The local axial strain in these aligned cell walls matches the applied macroscopic

strain (see Fig. 2a). This equivalence of local and macroscopic strains indicates maximal resistance to uniaxial loading (although, for arbitrary loading directions, the local and macroscopic strains may not necessarily be equivalent in the Kagome truss). The remaining cell walls undergo rigid-body motion to accommodate the overall deformation, meaning that only the cell walls aligned with the loading direction—comprising one-third of the total cell walls—bear the load.

In 2D, isotropy of the elasticity tensor requires three-fold structural symmetry [5, 6]. Consequently, for an isotropic 2D lattice, at most one-third of the cell walls can contribute to carrying uniaxial loads along a symmetry axis. The fact that the maximum number of cell walls allowed by isotropy stretch to the maximum possible strain (i.e., the applied macroscopic strain) renders the Young's modulus of the Kagome truss the upper bound for 2D lattices: $E/E_s \leq \bar{\rho}/3$.

Hydrostatic loading is analogous to uniaxial loading applied uniformly in all directions, and pure shear corresponds to the combined uniaxial tension and uniaxial compression in two mutually perpendicular directions. It is therefore evident that the Kagome truss attains the upper bound for all three elastic moduli.

Equations (2) through (5) demonstrate that isotropic materials are characterised by only two independent elastic constants. This indicates that an isotropic truss exhibiting a Poisson's ratio different from that of the Kagome truss can achieve equivalence with the Kagome truss in only one elastic modulus, while being inferior in the remaining two. Consequently, a 2D isotropic truss where $\nu \neq 1/3$ exhibits a suboptimal distribution of the solid phase, resulting in a reduced proportion of load-bearing cell walls under specific loading conditions at low relative densities.

Variational methods used to derive upper bounds on the elastic moduli, including those of Hashin and Shtrikman, rely on the assumption of an optimal distribution of solid material that maximizes load-bearing capacity under all loading conditions. For low-density 2D lattices, this results in $\nu_{\text{HS-min}} = \nu_{\text{HS}} = \nu_{\text{HS-max}} = 1/3$, reflecting the

most efficient material arrangement. Similarly, $\nu_{\text{HS-min}} \leq v \leq \nu_{\text{HS-max}}$ defines the range of Poisson's ratio where the composite maintains an optimal solid phase distribution. However, this does not preclude the determination of upper bounds for $v < \nu_{\text{HS-min}}$ or $v > \nu_{\text{HS-max}}$, as explained below.

Equation (A2) illustrates that G_{SH} is inversely proportional to ν_{s}, reaching its peak value at $\nu_{\text{HS-min}}$ (specifically, at $\nu_{\text{HS}}|_{\nu_{\text{s}}\to-1}$). Concurrently, the isotropy relation $G = E/(2+2v)$ demonstrates that G increases as ν decreases, thus achieving its maximum when $\nu \to -1$. These two principles, when considered in tandem, establish that $G_{\text{HS}}|_{\nu_{\text{s}}\to-1}$ serves as a rigorous upper bound for the shear modulus within the composite's Poisson's ratio range from -1 to $\nu_{\text{HS-min}}$. The corresponding upper bounds for Young's modulus and bulk modulus can subsequently be determined employing the isotropy relations specified in in equations (2) and (4).

In a parallel manner, equation (A3) demonstrates that K_{HS} is a monotonically increasing function of ν_{s}, reaching its maximum at $\nu_{\text{HS-max}}$ (i.e., when $\nu_{\text{s}} \to 0.5$). Additionally, the isotropy relation $K = E/(2-2v)$ dictates that K attains its maximum as ν approaches 0.5. The confluence of these two conditions establishes that $K_{\text{HS}}|_{\nu_{\text{s}}\to0.5}$ serves as a rigorous upper bound for the bulk modulus within the composite's Poisson's ratio range from $\nu_{\text{HS-max}}$ to 0.5. The corresponding upper bounds for Young's modulus and shear modulus can be derived through the application of the isotropy relations elucidated in equations (3) and (4).

Considering the aforementioned factors, the upper limits of the elastic moduli for two-phase solid-void isotropic materials in 2D can be expressed for any given combination of $0 \leq \rho \leq 1$ and $-1 < \nu < 1$. For $-1 < \nu \leq \nu_{\text{HS-min}}$:

$$\frac{G_{\text{NUB}}}{E_{\text{s}}} = \frac{G_{\text{HS}}}{E_{\text{s}}}\Big|_{\nu_{\text{s}}\to-1} = \frac{\bar{\rho}}{8\,(1-\bar{\rho})}, \tag{A5}$$

$$\frac{E_{\text{NUB}}}{E_{\text{s}}} = 2\,(1+\nu)\,G_{\text{NUB}}, \tag{A6}$$

$$\frac{K_{\text{NUB}}}{E_{\text{s}}} = \frac{1+\nu}{1-\nu}\,G_{\text{NUB}}, \tag{A7}$$

when $\nu_{\text{HS-min}} \leq \nu \leq \nu_{\text{HS-max}}$:

$$\nu_{\text{s}} = \frac{(1-2\nu)\,\bar{\rho} - (1-3\nu)}{\bar{\rho}}, \tag{A8}$$

$$\frac{E_{\text{NUB}}}{E_{\text{s}}} = \frac{E_{\text{HS}}}{E_{\text{s}}} = \frac{\bar{\rho}}{3-2\,\bar{\rho}}, \tag{A9}$$

$$\frac{G_{\text{NUB}}}{E_{\text{s}}} = \frac{G_{\text{HS}}}{E_{\text{s}}} = \frac{\bar{\rho}}{8-4\,\bar{\rho}(1+\nu)-2\,(1-3\nu)}, \tag{A10}$$

$$\frac{K_{\text{NUB}}}{E_{\text{s}}} = \frac{K_{\text{HS}}}{E_{\text{s}}} = \frac{\bar{\rho}}{4-4\,\bar{\rho}(1-\nu)+2\,(1-3\nu)}, \tag{A11}$$

and for $\nu_{\text{HS-max}} \leq \nu < 1$:

$$\frac{K_{\text{NUB}}}{E_{\text{s}}} = \frac{K_{\text{HS}}}{E_{\text{s}}}\Big|_{\nu_{\text{s}}\to 0.5} = \frac{\bar{\rho}}{4-3\,\bar{\rho}}, \tag{A12}$$

$$\frac{E_{\text{NUB}}}{E_{\text{s}}} = 2\,(1-\nu)\,K_{\text{NUB}}, \tag{A13}$$

$$\frac{G_{\text{NUB}}}{E_{\text{s}}} = \frac{1-\nu}{1+\nu}\,K_{\text{NUB}}, \tag{A14}$$

Supplementary Figs. 1b-d illustrate the evolution of the upper limits of the elastic moduli as functions of ν for $\bar{\rho}$ values of 0.75, 0.50, and 0.25. As $\bar{\rho}$ approaches zero, these upper bounds converge to those outlined in equation (6); see also Fig. 1a.

A2. 3D materials

Supplementary Fig. 2a illustrates the relationship between ν_{HS} and ν_{s} for various $\bar{\rho}$ values (equation A18) in 3D solid-void composites. As in the 2D case, ν_{HS} covers the entire thermodynamically feasible range of Poisson's ratio in 3D, from -1 to 0.5, but only when $\bar{\rho} = 1$. For $\bar{\rho}$ values below 1, the highest ν_{HS} is less than 0.5, decreasing further as $\bar{\rho}$ decreases (compare Supplementary Figs. 2b and 2c). Employing the same methodology used for 2D, the upper bounds on the elastic moduli for two-phase solid-void isotropic materials in 3D can be expressed for any given pair of $0 \leq \rho \leq 1$ and $-1 < \nu < 0.5$. For $-1 < \nu \leq \nu_{\text{HS-max}}$:

$$\frac{E_{\text{NUB}}}{E_{\text{s}}} = \frac{E_{\text{HS}}}{E_{\text{s}}} = \frac{2\,(7-5\,\nu_{\text{s}})\,\bar{\rho}}{3\,(1-\nu_{\text{s}})\,(9+5\,\nu_{\text{s}}) - \bar{\rho}\,(1+\nu_{\text{s}})\,(13-15\,\nu_{\text{s}})}, \tag{A15}$$

$$\frac{G_{\mathrm{NUB}}}{E_{\mathrm{s}}} = \frac{G_{\mathrm{HS}}}{E_{\mathrm{s}}} = \frac{(7-5\nu_{\mathrm{s}})\,\bar{\rho}}{2\,(1+\nu_{\mathrm{s}})\Big(15\,(1-\nu_{\mathrm{s}}) - \bar{\rho}\,(8-10\,\nu_{\mathrm{s}})\Big)} \tag{A16}$$

$$\frac{K_{\mathrm{NUB}}}{E_{\mathrm{s}}} = \frac{K_{\mathrm{HS}}}{E_{\mathrm{s}}} = \frac{2\,\bar{\rho}}{3\Big(3\,(1-\nu_{\mathrm{s}}) - \bar{\rho}\,(1+\nu_{\mathrm{s}})\Big)}, \tag{A17}$$

$$\nu_{\mathrm{HS}} = \frac{2\,(1+\nu_{\mathrm{s}})\Big(15\,(1-\nu_{\mathrm{s}}) - \bar{\rho}\,(8-10\,\nu_{\mathrm{s}})\Big)}{3\,(1-\nu_{\mathrm{s}})\,(9+5\,\nu_{\mathrm{s}}) - \bar{\rho}\,(1+\nu_{\mathrm{s}})\,(13-15\,\nu_{\mathrm{s}})} - 1, \tag{A18}$$

$$\nu_{\mathrm{s}} = \frac{6\,(1+\nu) + \bar{\rho}\,(1-\nu) - \sqrt{9\,(3-7\,\nu)^2 - 12\,\bar{\rho}\,(4-35\,\nu+51\,\nu^2) + 4\,\bar{\rho}^2\,(2-7\,\nu)^2}}{5\Big(3\,(1-\nu) - \bar{\rho}\,(1-3\,\nu)\Big)}, \tag{A19}$$

and for $\nu_{\text{HS-max}} \leq \nu < 0.5$:

$$\frac{K_{\mathrm{NUB}}}{E_{\mathrm{s}}} = \frac{K_{\mathrm{HS}}}{E_{\mathrm{s}}}\,|_{\nu_{\mathrm{s}}\to 0.5} = \frac{4\,\bar{\rho}}{9\,(1-\bar{\rho})}, \tag{A20}$$

$$\frac{E_{\mathrm{NUB}}}{E_{\mathrm{s}}} = 3\,(1-2\,\nu)\,K_{\mathrm{NUB}}, \tag{A21}$$

$$\frac{G_{\mathrm{NUB}}}{E_{\mathrm{s}}} = \frac{3\,(1-2\,\nu)}{2\,(1+\nu)}\,K_{\mathrm{NUB}}, \tag{A22}$$

A comparative analysis of Supplementary Figs. 2 and 3 reveal substantial disparities between the 2D and 3D solid-void composites. In 3D, ν_{HS} encompasses the entire spectrum of negative Poisson's ratios irrespective of the $\bar{\rho}$ value. Furthermore, the upper bound of the shear modulus in the negative Poisson's ratio regime continuously increases as ν decreases, approaching infinity as ν tends towards -1 for all $\bar{\rho}$ values. Conversely, this behaviour is observed exclusively at $\bar{\rho} = 1$ in the 2D composites.

Another significant distinction lies in the nature of the material represented by $\bar{\rho} \to 0$ in different dimensions. In 2D, $\bar{\rho} \to 0$ corresponds to interconnected beam networks or truss lattices, whereas in 3D, $\bar{\rho} \to 0$ allows for both closed-cell (such as plate and shell lattices) and open-cell (such as truss lattices) configurations. The variational formulation of Hashin and Shtrikman does not differentiate between closed- and open-cell materials. Consequently, the HS upper bounds effectively correspond to closed-cell materials, which are generally stiffer than open-cell materials. The HS upper bounds for $\bar{\rho} \to 0$ and $-1 < \nu \leq \nu_{\text{HS-max}}$ reduce to:

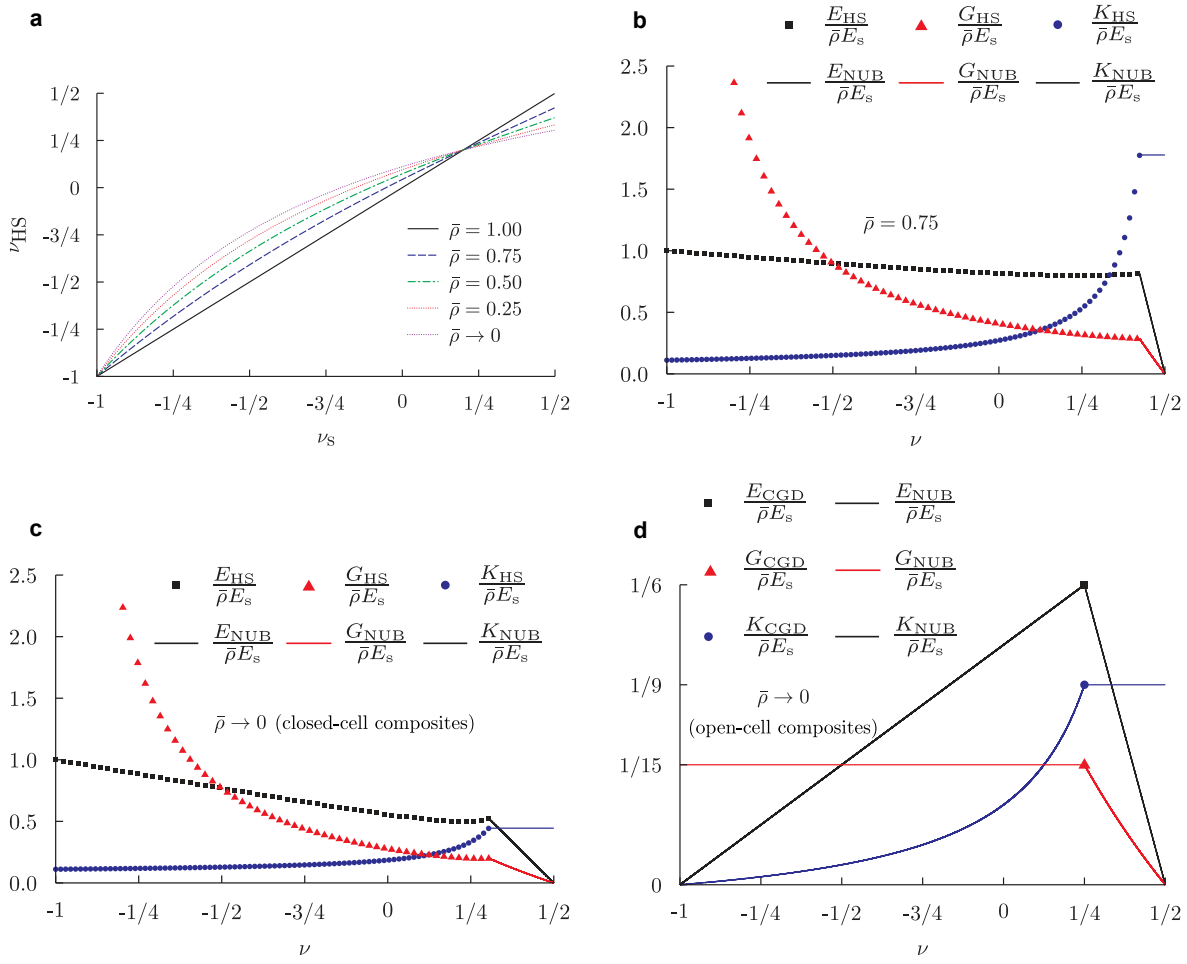

Supplementary Fig. 2 | Upper bounds on the elastic moduli of three-dimensional two-phase solid-void isotropic composites. a, Variation of ν_{HS} (Poisson's ratio of a composite adhering to the HS upper bounds for a specific combination of relative density, $\bar{\rho}$, and solid material Poisson's ratio, ν_s; see equation A18), as a function of ν_s. **b-d,** Evolution of the upper bounds for Young's modulus, shear modulus, and bulk modulus as functions of the composite Poisson's ratio, ν, for: **b,** composites with $\bar{\rho} = 0.75$ (equations A15-A22); **c,** closed-cell composites in the limit $\bar{\rho} \to 0$ (equations A23-A30), and **d,** open-cell composites in the limit $\bar{\rho} \to 0$ (equations A31-A36).

$$\frac{E_{NUB}}{E_s} = \frac{E_{HS}}{E_s} = \frac{2(7-5\nu_s)\bar{\rho}}{3(1-\nu_s)(9+5\nu_s)}, \tag{A23}$$

$$\frac{G_{NUB}}{E_s} = \frac{G_{HS}}{E_s} = \frac{(7-5\nu_s)\bar{\rho}}{30(1-\nu_s^2)} \tag{A24}$$

$$\frac{K_{NUB}}{E_s} = \frac{K_{HS}}{E_s} = \frac{2\bar{\rho}}{9(1-\nu_s)}, \tag{A25}$$

$$\nu_{\text{HS}} = \frac{1+5\,\nu_{\text{s}}}{9+5\,\nu_{\text{s}}}, \tag{A26}$$

$$\nu_{\text{s}} = \frac{9\,\nu-1}{5\,(1-\nu)}, \tag{A27}$$

and for $\nu_{\text{HS-max}} \leq \nu < 0.5$:

$$\frac{K_{\text{NUB}}}{E_{\text{s}}} = \frac{K_{\text{HS}}}{E_{\text{s}}}\,|_{\nu_{\text{s}}\to 0.5} = \frac{4\,\bar{\rho}}{9}, \tag{A28}$$

$$\frac{E_{\text{NUB}}}{E_{\text{s}}} = 3\,(1-2\,\nu)\,K_{\text{NUB}}, \tag{A29}$$

$$\frac{G_{\text{NUB}}}{E_{\text{s}}} = \frac{3\,(1-2\,\nu)}{2\,(1+\nu)}\,K_{\text{NUB}}, \tag{A30}$$

Christensen [3] and Gurtner and Durand [4] derived more stringent upper bounds for open-cell composites (or truss lattices) by constraining the solid distribution in the composite to slender struts. As in the 2D case, these upper bounds, derived from variational principles, are limited to a single value of the composite's Poisson's ratio, $\nu = 0.25$ in 3D. Here, we extend these bounds to encompass the full range of Poisson's ratios. For $-1 < \nu \leq 0.25$:

$$\frac{G_{\text{NUB}}}{E_{\text{s}}} = \frac{G_{\text{CGD}}}{E_{\text{s}}} = \frac{\bar{\rho}}{15}, \tag{A31}$$

$$\frac{E_{\text{NUB}}}{E_{\text{s}}} = 2\,(1+\nu)\,G_{\text{NUB}}, \tag{A32}$$

$$\frac{K_{\text{NUB}}}{E_{\text{s}}} = \frac{1+\nu}{1-\nu}\,G_{\text{NUB}}, \tag{A33}$$

and for $0.25 \leq \nu < 0.5$:

$$\frac{K_{\text{NUB}}}{E_{\text{s}}} = \frac{K_{\text{HS}}}{E_{\text{s}}} = \frac{\bar{\rho}}{9}, \tag{A34}$$

$$\frac{E_{\text{NUB}}}{E_{\text{s}}} = 2\,(1-\nu)\,K_{\text{NUB}}, \tag{A35}$$

$$\frac{G_{\text{NUB}}}{E_{\text{s}}} = \frac{1-\nu}{1+\nu}\,K_{\text{NUB}}, \tag{A36}$$

The evolution of the upper bounds on the elastic moduli as a function of ν for both closed- and open-cell composites in the limit of $\bar{\rho} \to 0$ is shown in Supplementary Figs. 2c and 2d, respectively.

A3. Hierarchical lattices

In hierarchical or multiscale lattices, each strut is composed of a smaller-scale lattice [7]. Let the mechanical properties of the larger-scale lattice be denoted by the subscript "1" and those of the smaller-scale lattice by "2". The overall relative density of the composite is thus given by $\bar{\rho} = \bar{\rho}_1 \bar{\rho}_2$. For $\bar{\rho}_2 \to 0$ (implying $\bar{\rho} \to 0$), Poisson's ratio of the cell wall, $\nu_s = \nu_2$, can span the full theoretical range from -1 to 1, regardless of whether the composite is a 2D or 3D material. In the limit of dilute relative density ($\bar{\rho} \ll 1$), the upper bounds of the elastic moduli for truss lattices, in both 2D and 3D, remain independent of ν_s. Thus, hierarchy has no impact on the upper bounds of truss lattices. However, this principle does not apply to 3D plate or shell lattices, as evidenced in equations (A23)-(A30).

For low-density 3D plate or shell lattices, shifting the upper limit of ν_s from 0.5 to 1 increases $\nu_{\text{HS-max}}$ from 0.304 to 0.429 (equation A26). This shift enables the upper bounds for all three elastic moduli (equations A23-A25) to grow significantly as ν approaches $\nu_{\text{HS-max}}$ (i.e., as $v_s \to 1$). However, the moduli remain finite since ν_s can approach but never attain 1. In the regime where $\nu_{\text{HS-max}} \leq \nu < 0.5$, the upper bounds simplify to:

$$\frac{K_{\text{NUB}}}{E_s} = \frac{K_{\text{HS}}}{E_s}\Big|_{\nu_s \to 1} \gg 1, \tag{A37}$$

$$\frac{E_{\text{NUB}}}{E_s} = 3(1-2\nu)\,K_{\text{NUB}}, \tag{A38}$$

$$\frac{G_{\text{NUB}}}{E_s} = \frac{3(1-2\nu)}{2(1+\nu)}\,K_{\text{NUB}}, \tag{A39}$$

Equations (A37)-(A39) demonstrates that increasing ν beyond $\nu_{\text{HS-max}}$ does not alter K_{NUB}, which remains significantly larger than E_s. Concurrently, E_{NUB} and G_{NUB} decrease continuously as ν increases, with $E_{\text{NUB}} \to 3G_{\text{NUB}} \to 0$ as ν approaches 0.5.

In our derivation of upper bounds for isotropic materials, encompassing two-dimensional, three-dimensional, and hierarchical materials, we allowed the Poisson's ratio of the composite ν to fall below $\nu_{\text{HS-min}}$ or exceed $\nu_{\text{HS-max}}$, where ν is independent of the solid

material's Poisson's ratio ν_s. This approach involves an implicit assumption that any thermodynamically permissible ν value can be achieved in two-phase solid-void composites through appropriate engineering of the solid phase distribution, regardless of the relative density $\bar{\rho}$. While this assumption holds for low-density lattices, it remains subject to scrutiny for high-density composites. Our analysis of various lattices reveals that ν deviates from the extremes of -1 and 1 as $\bar{\rho}$ increases. For instance, the Poisson's ratio of the hexagonal lattice, which approaches 1 in the low-density limit, decreases with increasing $\bar{\rho}$, falling below 0.5 for $\bar{\rho} > 0.5$ [8, 9]. It is therefore imperative to note that the existence of upper bounds on elastic properties does not necessarily imply the availability of materials that achieve these bounds. Nonetheless, these findings offer insights that may guide future efforts in designing stiff, lightweight materials, broadening potential directions for material innovation.

B. Mechanical properties and mechanisms of infinite periodic trusses trough matrix methods

In the regime of low relative density ($\bar{\rho} \ll 1$), the mechanical behaviour of an infinite periodic pin-jointed truss closely mirrors that of a rigid-jointed lattice. This correspondence enables a simplified mathematical analysis of the lattice's mechanical properties by using the less complex truss model as a proxy.

Seminal papers by Pellegrino and Calladine [10] and Pellegrino [11] established methods for identifying inextensional mechanisms and self-stress states in finite pin-jointed truss structures using equilibrium matrix analysis. These methods were subsequently expanded by Deshpande et al. [12], Guest and Hutchinson [13], and Hutchinson and Fleck [14] for application to infinite periodic trusses.

Ickin and Tekoğlu [15] recently enhanced existing matrix methods to derive closed-form expressions for the mechanical properties of lattice materials. They also introduced an innovative finite element method-based approach to identify self-stress states and infinitesimal mechanisms in periodic trusses under specific uniform macroscopic loading conditions (used to create Fig. 2 of this study). This research adopts the methodologies

outlined in [15]. Below, we elucidate the key steps of the matrix methods as applied to infinite periodic twisted Kagome trusses. Additionally, we provide MATLAB [16] codes implementing the matrix methods for twisted Kagome (Appendix A), hexachiral (Appendix B), and Double Triangular trusses (Appendix C). The unit cells of these trusses, used in the matrix analysis, are shown in Supplementary Fig. 3 (see also Fig. 1 and Extended Data Fig. 1). For more comprehensive information on matrix methods, readers are referred to Ickin and Tekoğlu [15] and the references therein.

An infinite, periodic, pin-jointed twisted Kagome truss can be generated by translating the unit cell shown in Supplementary Fig. 3a using the direct lattice translation vector $\boldsymbol{x} = n^k \boldsymbol{a}_k$, where n^k denotes any set of integer values. The translation basis is defined as $\boldsymbol{a}_k = \Big(\cos(k\pi/3)\boldsymbol{i} + \sin(k\pi/3)\boldsymbol{j}\Big) 2\cos(\theta) L$, with $k \in \{1, 2\}$, and $\boldsymbol{i}$ and $\boldsymbol{j}$ being unit vectors along the x_1 and x_2 axes, respectively. Under a periodic displacement field, the displacement difference between homologous boundary joint pairs is given by:

$$\begin{aligned} d_k^{(2)} - d_k^{(5)} &= \Big(\cos(\pi/3)E_{k1} + \sin(\pi/3)E_{k2}\Big) 2\cos(\theta) L, \\ d_k^{(4)} - d_k^{(3)} &= \Big(\cos(\pi/3)E_{k1} - \sin(\pi/3)E_{k2}\Big) 2\cos(\theta) L, \end{aligned} \tag{B1}$$

where $d_k^{(i)}$ is the displacement of the i'th joint along the k-axis direction, and E_{k1} and E_{k2} are the components of the macroscopically homogeneous strain field $\boldsymbol{E}$ imposed on the pin-jointed truss. Bar elongations can be determined from joint displacements through the relation:

$$\mathbf{B} \cdot \boldsymbol{d} = \boldsymbol{e}, \tag{B2}$$

where $\mathbf{B}$ is the kinematic matrix, $\boldsymbol{d}$ is the joint displacement vector, $\boldsymbol{e}$ is the bar elongation vector. For the twisted Kagome trusses:

$$\boldsymbol{d}^{\mathrm{T}} = \begin{bmatrix} d_1^{(1)} & d_2^{(1)} & d_1^{(2)} & d_2^{(2)} & d_1^{(3)} & d_2^{(3)} & d_1^{(4)} & d_2^{(4)} & d_1^{(5)} & d_2^{(5)} & d_1^{(6)} & d_2^{(6)} \end{bmatrix}, \tag{B3}$$

$$\boldsymbol{e}^{\mathrm{T}} = \begin{bmatrix} e_1 & e_2 & e_3 & e_4 & e_5 & e_6 \end{bmatrix}, \tag{B4}$$

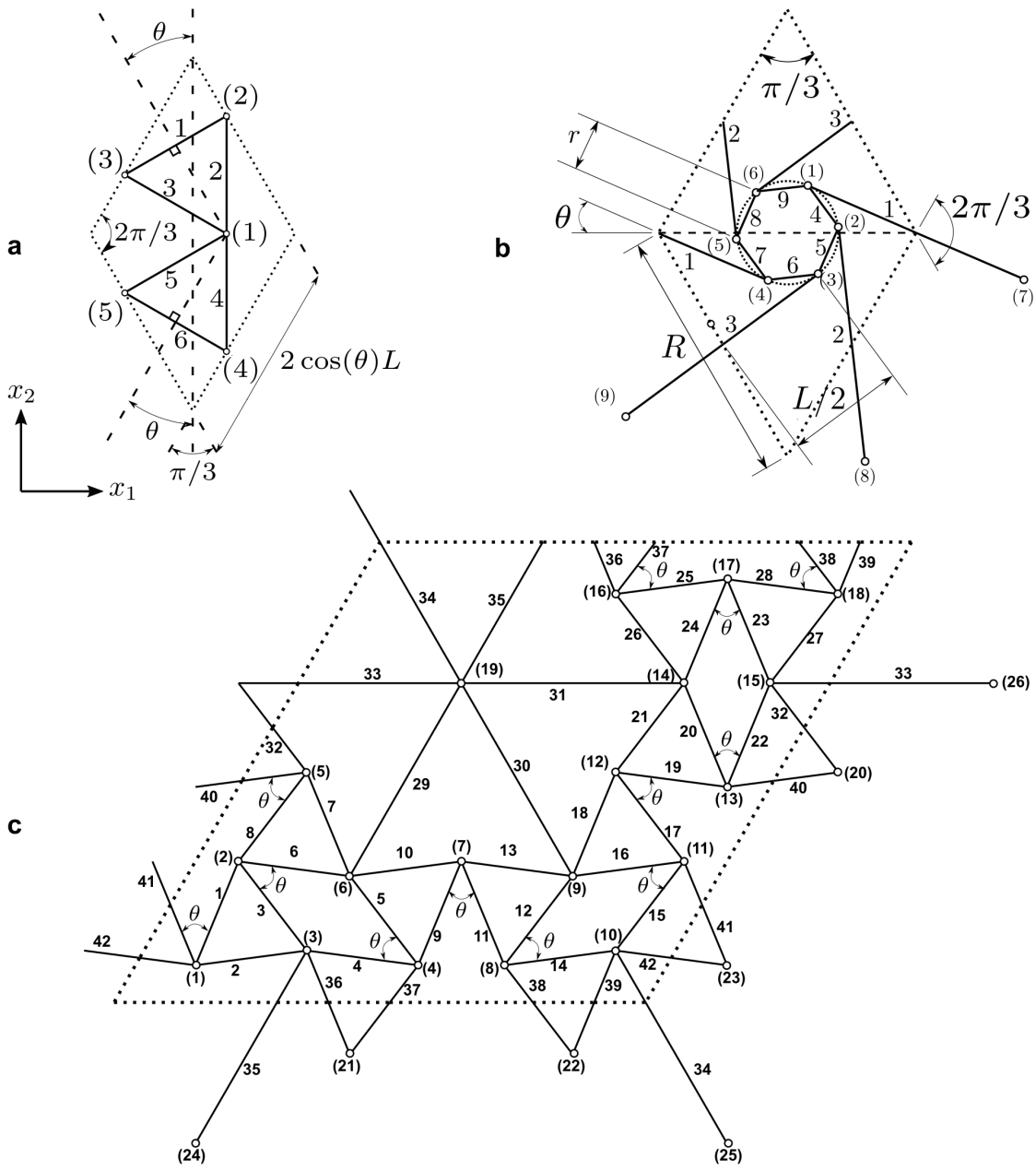

Supplementary Fig. 3 | Node and bar numbering scheme of the unit cells for matrix analysis. Illustrations of unit cells with corresponding node and bar numbering schemes for three types of infinite periodic pin-jointed trusses: **a,** twisted Kagome ($0° < \theta < 60°$); **b,** hexachiral ($0° < \theta < 90°$); and **c,** Double Triangular ($0° < \theta < 180°$). Empty circles represent the joints where the cell walls meet, and unit cell boundaries are indicated by dotted lines.

$$\mathbf{B}^{\mathrm{T}} = \begin{bmatrix} 0 & -\cos(\theta+\pi/3) & \cos(\theta-\pi/3) & -\cos(\theta+\pi/3) & \cos(\theta-\pi/3) & 0 \\ 0 & -\cos(\theta-\pi/6) & -\cos(\theta+\pi/6) & \cos(\theta-\pi/6) & \cos(\theta+\pi/6) & 0 \\ \cos(\theta) & \cos(\theta+\pi/3) & 0 & 0 & 0 & 0 \\ \cos(\theta-\pi/2) & \cos(\theta-\pi/6) & 0 & 0 & 0 & 0 \\ -\cos(\theta) & 0 & -\cos(\theta-\pi/3) & 0 & 0 & 0 \\ -\cos(\theta-\pi/2) & 0 & \cos(\theta+\pi/6) & 0 & 0 & 0 \\ 0 & 0 & 0 & \cos(\theta+\pi/3) & 0 & \cos(\theta) \\ 0 & 0 & 0 & -\cos(\theta-\pi/6) & 0 & -\cos(\theta-\pi/2) \\ 0 & 0 & 0 & 0 & -\cos(\theta-\pi/3) & -\cos(\theta) \\ 0 & 0 & 0 & 0 & -\cos(\theta+\pi/6) & \cos(\theta-\pi/2) \end{bmatrix}, \tag{B5}$$

where the superscript T denotes the transpose operator.

Substituting the periodicity relations (B1) into the unit cell kinematic relation $\mathbf{B} \cdot \boldsymbol{d} = \boldsymbol{e}$ results in the reduced kinematic statement $\bar{\mathbf{B}} \cdot \bar{\boldsymbol{d}} = \bar{\boldsymbol{e}}$ for the infinite, pin-jointed, twisted Kagome truss, where:

$$\bar{\mathbf{B}}^{\mathrm{T}} = \begin{bmatrix} 0 & -\cos(\theta+\pi/3) & \cos(\theta-\pi/3) & -\cos(\theta+\pi/3) & \cos(\theta-\pi/3) & 0 \\ 0 & -\cos(\theta-\pi/6) & -\cos(\theta+\pi/6) & \cos(\theta-\pi/6) & \cos(\theta+\pi/6)) & 0 \\ \cos(\theta) & \cos(\theta+\pi/3) & 0 & 0 & -\cos(\theta-\pi/3) & -\cos(\theta) \\ \cos(\theta-\pi/2) & \cos(\theta-\pi/6) & 0 & 0 & -\cos(\theta+\pi/6) & \cos(\theta-\pi/2) \\ -\cos(\theta) & 0 & -\cos(\theta-\pi/3) & \cos(\theta+\pi/3) & 0 & \cos(\theta) \\ -\cos(\theta-\pi/2) & 0 & \cos(\theta+\pi/6) & -\cos(\theta-\pi/6) & 0 & -\cos(\theta-\pi/2) \end{bmatrix}, \tag{B6}$$

$$\bar{\boldsymbol{d}}^{\mathrm{T}} = \begin{bmatrix} d_1^{(1)} & d_2^{(1)} & d_1^{(2)} & d_2^{(2)} & d_1^{(3)} & d_2^{(3)} \end{bmatrix}, \tag{B7}$$

$$\bar{\boldsymbol{e}}^{\mathrm{T}} = \begin{bmatrix} e_1 & e_2 & e_3 & e_4 + g_4(\boldsymbol{E},\theta) & e_5 + g_5(\boldsymbol{E},\theta) & e_6 + g_6(\boldsymbol{E},\theta) \end{bmatrix}, \tag{B8}$$

with

$$\begin{aligned} g_4(\boldsymbol{E},\theta) = \Big(& \cos(\theta)\ \big(E_{11} + 3E_{22} - 2\sqrt{3}E_{12}\big) - \\ & \cos(\theta - \pi/2)\ \big(\sqrt{3}E_{11} - \sqrt{3}E_{22} - 2E_{12}\big)\Big)\ \cos(\theta)L/2, \end{aligned} \tag{B9}$$

$$\begin{aligned} g_5(\boldsymbol{E},\theta) = \Big(& \cos(\theta)\ \big(E_{11} + 3E_{22} + 2\sqrt{3}E_{12}\big) + \\ & \cos(\theta - \pi/2)\ \big(\sqrt{3}E_{11} - \sqrt{3}E_{22} + 2E_{12}\big)\Big)\ \cos(\theta)L/2, \end{aligned} \tag{B10}$$

$$g_6(\boldsymbol{E},\theta) = \Big(\cos(\theta)\ E_{11} - \cos(\theta - \pi/2)\ E_{12} \Big)\ 2\cos(\theta)L. \tag{B11}$$

The conjugate reduced equilibrium relation is $\bar{\mathbf{A}} \cdot \bar{\boldsymbol{t}} = \mathbf{0}$, where $\bar{\mathbf{A}}$ denotes the reduced equilibrium matrix and $\bar{\boldsymbol{t}}$ denotes the reduced bar tension vector. The principle of virtual work entails $\bar{\mathbf{A}} = \bar{\mathbf{B}}^{\mathrm{T}}$, and the null space of $\bar{\mathbf{A}}$, $\boldsymbol{Z} = \mathrm{Null}(\bar{\mathbf{A}}) = \mathrm{Null}(\bar{\mathbf{B}}^{\mathrm{T}})$, is a linearly independent basis spanning all the reduced bar tension vectors $\bar{\boldsymbol{t}}$ compatible with unit cell-periodic states of self-stress. For the twisted Kagome trusses:

$$\boldsymbol{Z}^{\mathrm{T}} = \begin{bmatrix} 2\sqrt{3}\sin(2\theta)/3 & 2\sqrt{3}\cos(2\theta+\pi/6)/3 & -2\sqrt{3}\sin(2\theta+\pi/3)/3 & -1 & 1 & 0 \\ 2\sqrt{3}\sin(2\theta+\pi/3)/3 & -2\sqrt{3}\sin(2\theta)/3 & -2\sqrt{3}\cos(2\theta+\pi/6)/3 & -1 & 0 & 1 \end{bmatrix}. \tag{B12}$$

It is important to emphasize that each column of the $\boldsymbol{Z}$ matrix represents the relative tension in each bar for an independent state of bar tensions. For any macroscopic stress state (where the loading is applied at infinity on the infinite periodic truss, resulting in zero nodal forces), the bar tensions must conform to a linear combination of these independent tension states. This ensures that the bar tensions satisfy the equilibrium conditions dictated by the macroscopic stress field.

The bar tension ratios provided by the $\boldsymbol{Z}$ matrix can be expressed through a system of linear homogeneous equations:

$$\boldsymbol{Q}_{(l-n)\times l}\ \boldsymbol{Z}_{n\times l} = \mathbf{0}. \tag{B13}$$

In this context, l represents the total number of bars in the unit cell, while n denotes the number of independent self-stress states (for twisted Kagome trusses, $l = 6$ and $n = 2$). The matrix $\boldsymbol{Q}$ is defined as the transpose of the left null space of $\boldsymbol{Z}$, expressed as:

$$\boldsymbol{Q} = \left(\text{Null}\left(\boldsymbol{Z}^{\mathrm{T}}\right)\right)^{\mathrm{T}}. \tag{B14}$$

Given that the bar tensions $\boldsymbol{t}$ corresponding to any macroscopic stress state must be a linear combination of the columns in the $\boldsymbol{Z}$ matrix, one can express:

$$\boldsymbol{Q}\boldsymbol{t} = \boldsymbol{0}. \tag{B15}$$

In this study, we assume, without loss of generality, that all l bars in the unit cell possess identical axial rigidity $E_{\mathrm{s}}A$. When expressing bar tensions in terms of bar elongations ($t_l = E_{\mathrm{s}}Ae_l/L_l$, no summation on l), equation (B15) simplifies to:

$$\boldsymbol{Q}\boldsymbol{e}^{(L)} = \boldsymbol{0}, \tag{B16}$$

where each element of $\boldsymbol{e}^{(L)}$ corresponds to the elongation of the of the lth bar relative to its length, i.e., e_l/L_l. To rewrite equation (B16) in terms of $\boldsymbol{e}$, the bar lengths are absorbed into the $\boldsymbol{Q}$ matrix, resulting in:

$$\boldsymbol{P}_{4\times 6}\ \boldsymbol{e}_{6\times 1} = \boldsymbol{0}. \tag{B17}$$

Here, $P_{ij} = Q_{ij}(L_u/L_j)$, with $L_u = L$ as the unit bar length, and no summation over j. Since the right-hand side remains zero, multiplying by L_u does not affect equation (B17) but ensures that the components of the $\boldsymbol{P}$ matrix are dimensionless. For twisted Kagome trusses, where the bar lengths are uniform ($L_j = L_u = L$), P_{ij} simplifies to Q_{ij}. However, this equivalence does not hold for structures with non-uniform bar lengths, such as Double Triangular trusses (see Appendix C for details).

The twisted Kagome unit cell comprises six bars; however, (B17) provides only four equations. The remaining two equations for the bar elongations $\boldsymbol{e}$ can be derived by by recognising that the $\boldsymbol{Z}$ matrix is the left null space of the reduced kinematic matrix $\bar{\boldsymbol{B}}$ and that $\bar{\boldsymbol{e}} = \boldsymbol{e} - \boldsymbol{g}(\boldsymbol{E})$:

$$\boldsymbol{Z}^{\mathrm{T}}\bar{\boldsymbol{B}}\bar{\boldsymbol{d}} = \boldsymbol{Z}^{\mathrm{T}}\bar{\boldsymbol{e}} = \boldsymbol{0}$$

$$\Longrightarrow \boldsymbol{Z}^{\mathrm{T}}\boldsymbol{e} = \boldsymbol{Z}^{\mathrm{T}}\boldsymbol{g}(\boldsymbol{E}). \tag{B18}$$

Combining (B17) and (B18) into one set of equations provides the complete set of equations for $\boldsymbol{e}$:

$$\left[\begin{array}{c} \boldsymbol{P} \\ \hline \boldsymbol{Z}^{\mathrm{T}} \end{array}\right] \boldsymbol{e} = \left[\begin{array}{c} \boldsymbol{0} \\ \hline \boldsymbol{Z}^{\mathrm{T}}\boldsymbol{g}(\boldsymbol{E}) \end{array}\right], \tag{B19}$$

where the horizontal line between matrices (and vectors) denotes matrix concatenation operation. For the twisted Kagome lattices, equation (B19) reduces to:

$$\begin{bmatrix} 1 & 1 & 1 & 0 & 0 & 0 \\ 2\sqrt{3}\sin(2\theta+\pi/3)/3 & 2\sqrt{3}\cos(2\theta+\pi/6)/3 & 0 & 1 & 0 & 0 \\ -2\sqrt{3}\sin(2\theta)/3 & -2\sqrt{3}\sin(2\theta+\pi/3)/3 & 0 & 0 & 1 & 0 \\ -2\sqrt{3}\cos(2\theta+\pi/6)/3 & 2\sqrt{3}\sin(2\theta)/3 & 0 & 0 & 0 & 1 \\ 2\sqrt{3}\sin(2\theta)/3 & 2\sqrt{3}\cos(2\theta+\pi/6)/3 & -2\sqrt{3}\sin(2\theta+\pi/3)/3 & -1 & 1 & 0 \\ 2\sqrt{3}\sin(2\theta+\pi/3)/3 & -2\sqrt{3}\sin(2\theta)/3 & -2\sqrt{3}\cos(2\theta+\pi/6)/3 & -1 & 0 & 1 \end{bmatrix} \begin{bmatrix} e_1 \\ e_2 \\ e_3 \\ e_4 \\ e_5 \\ e_6 \end{bmatrix} =$$

$$\begin{bmatrix} 0 \\ 0 \\ 0 \\ 0 \\ \sqrt{3}/2\sin(2\theta)L\ (E_{11}-E_{22}) + \sqrt{3}(\cos(2\theta)+1)L\ E_{12} \\ (\sqrt{3}/2\sin(2\theta+\pi/3)+3/4)L\ (E_{11}-E_{22}) + \sqrt{3}(\cos(2\theta+\pi/3)+1/2)L\ E_{12} \end{bmatrix}. \tag{B20}$$

The last two equations in (B20) show that macroscopic strain producing ($\boldsymbol{E} \neq 0$) inextensional mechanisms ($\boldsymbol{e} = 0$) of the twisted Kagome lattices occur for the equibiaxial

strain state $E_{11} = E_{22}$ with $E_{12} = 0$, regardless of the twist angle. The collapse modes correspond to rigid-body rotations of the unit cell's two triangles at equal angles but in opposite directions, with node (1) serving as the rotation center (see Supplementary Fig. 3a). Bar elongations are derived by solving equation (B20):

$$
\begin{aligned}
e_1 &= (\cos(2\theta) + 1)\, L/4\ (E_{11} - E_{22}) + \sin(2\theta) L/2\ E_{12},\\
e_2 &= (\cos(2\theta - \pi/3)/4 + 1/8)\, L\ (E_{22} - E_{11}) + \left(\cos(2\theta + \pi/6)/2 + \sqrt{3}/4\right) L\ E_{12},\\
e_3 &= (\cos(2\theta + \pi/3)/4 + 1/8)\, L\ (E_{22} - E_{11}) - \left(\sin(2\theta + \pi/3)/2 + \sqrt{3}/4\right) L\ E_{12},\\
e_4 &= (\cos(2\theta - \pi/3)/4 + 1/8)\, L\ (E_{22} - E_{11}) - \left(\cos(2\theta + \pi/6)/2 + \sqrt{3}/4\right) L\ E_{12},\\
e_5 &= (\cos(2\theta + \pi/3)/4 + 1/8)\, L\ (E_{22} - E_{11}) + \left(\sin(2\theta + \pi/3)/2 + \sqrt{3}/4\right) L\ E_{12},\\
e_6 &= (\cos(2\theta) + 1)\, L/4\ (E_{11} - E_{22}) - \sin(2\theta) L/2\ E_{12}.
\end{aligned}
\tag{B21}
$$

The strain energy per unit area of the unit cell represented in Supplementary Fig. 3a is $W = t_l e_l/(2S)$, where S is the unit cell area calculated using $S = 2\sqrt{3}\cos^2(\theta)L^2$. The components of the macroscopic stiffness tensor $\bar{\boldsymbol{\mathcal{L}}}$ are thus given by:

$$
\boldsymbol{\mathcal{L}}_{\alpha\beta\gamma\delta} = \frac{\partial^2 W(\boldsymbol{E})}{\partial E_{\alpha\beta}\partial E_{\gamma\delta}} = \frac{E_s A}{LS}\frac{\partial e_l(\boldsymbol{E})}{\partial E_{\alpha\beta}}\frac{\partial e_l(\boldsymbol{E})}{\partial E_{\gamma\delta}} \quad \forall\ \alpha,\beta,\gamma,\delta \in \{1,2\}, \tag{B22}
$$

summed over $l \in \{1, 2, ..., 6\}$. By substituting the bar elongations from equation (B21) into equation (B22), the components of the macroscopic stiffness tensor for twisted Kagome lattices are obtained:

$$
\mathcal{L}_{1111} = \mathcal{L}_{2222} = -\mathcal{L}_{1122} = -\mathcal{L}_{2211} = \mathcal{L}_{1212} = \mathcal{L}_{2121} = \mathcal{L}_{1221} = \mathcal{L}_{2112} = \frac{\sqrt{3}}{8}\frac{E_s A}{L}, \tag{B23}
$$

irrespective of the twist angle θ. The elastic constants of the twisted Kagome lattices are derived as follows:

$$
\frac{E}{E_s} = \frac{\mathcal{L}_{1111}(1-\nu^2)}{E_s} = \frac{\mathcal{L}_{2222}(1-\nu^2)}{E_s} = 0, \tag{B24}
$$

$$
\frac{G}{E_s} = \frac{\mathcal{L}_{1212}}{E_s} = \frac{\cos^2(\theta)}{8}\bar{\rho}, \tag{B25}
$$

$$\nu = \frac{\mathcal{L}_{1122}}{\mathcal{L}_{2222}} = \frac{\mathcal{L}_{1122}}{\mathcal{L}_{1111}} = -1, \tag{B26}$$

where $\bar{\rho} = \sqrt{3}A/(\cos^2(\theta)L)$ is the first-order relative density of the twisted Kagome lattices. The fact that $\nu \to -1$ at $\bar{\rho} \to 0$ for twisted Kagome lattices can also be deduced as follows. Under uniaxial compression, for example, along the x_1-axis, the collapse mechanism of the pin-jointed twisted Kagome trusses is activated, where $E_{11} = E_{22}$ and $E_{12} = 0$, and consequently $\nu = -E_{22}/E_{11} = -1$.

Guest and Hutchinson [13] demonstrated that the null space of the augmented kinematic matrix, $\boldsymbol{B}^{\text{aug}}$, offers a linearly independent basis for the nodal displacements corresponding to infinitesimal mechanisms in an infinite periodic truss, regardless of whether they induce macroscopic strain (see also [17]). The MATLAB code provided in Appendix A illustrates this by calculating the relative nodal displacement ratios for a collapse mechanism under hydrostatic loading. These computed displacements are in perfect agreement with the finite element (FE) results shown in Fig. 2h.

Appendix B contains a MATLAB code for analyzing hexachiral lattices. Here, the hexachiral microarchitecture is characterized by the angle $\theta = \arctan(2r/L)$, instead of the $R_r = R/r$ ratio used in the main text, which simplifies the construction of the $\bar{\mathbf{B}}$ matrix. The analysis produces an empty $\boldsymbol{Z}$ matrix, irrespective of the θ value, indicating that infinite periodic hexachiral trusses exhibit macroscopic strain-producing collapse mechanisms under all loading conditions. Consequently, for $\bar{\rho} \ll 1$, hexachiral lattices are bending-dominated across all loading scenarios, in agreement with the results shown in Figs. 2m-p.

In contrast to the MATLAB codes for the twisted Kagome and hexachiral trusses, the MATLAB code for Double Triangular trusses, provided in Appendix C, cannot solve the equations if θ is defined symbolically. Therefore, the user must assign a specific θ value for each run. For all θ values except 60° and 145.66°, the null space of the $\boldsymbol{B}^{\text{aug}}$ matrix contains two columns, corresponding to the rigid body translations of the entire truss in the x_1 and x_2 directions, indicating redundancy and the absence of infinitesimal mechanisms, whether strain-producing or not. At $\theta = 60°$, the truss supports only shear

loading, while at $\theta = 145.66°$, it supports only hydrostatic loading. The MATLAB code calculates the relative nodal displacement ratios for collapse mechanisms under hydrostatic loading at $\theta = 60°$ and pure shear loading at $\theta = 145.66°$, with the results perfectly matching the FE simulations presented in Fig. 2.

C. Deformation mechanisms in lattice materials

The effective macroscopic elastic moduli of lattice materials can be expressed as power-law relationships in terms of the relative density $\bar{\rho}$ and the solid's Young's modulus E_s as follows:

$$\frac{E}{E_s} = A\bar{\rho}^a, \quad \frac{G}{E_s} = B\bar{\rho}^b, \quad \frac{K}{E_s} = C\bar{\rho}^c, \tag{C1}$$

where A, B, and C are functions of $\bar{\rho}$, Poisson's ratio ν, and the the lattice's microarchitecture. The exponents a, b, and c typically range from 1 to 3 in 2D lattices and from 1 to 2 in 3D lattices, with the lower bound corresponding to stretching-dominated behaviour and the upper bound to bending-dominated behaviour. In the limit of low relative density ($\bar{\rho} \to 0$), the exponents adopt boundary values of either 1 or 3 in 2D, and 1 or 2 in 3D [7].

For instance, in a 2D hexagonal lattice, which is bending-dominated under uniaxial and shear loading and stretching-dominated under hydrostatic loading, the exponents are $a = 3$, $b = 3$, and $c = 1$. If the elastic moduli and Poisson's ratio were entirely independent, there would be eight possible combinations of these exponents as $\bar{\rho} \to 0$, each representing distinct deformation mechanisms under uniaxial, shear, and hydrostatic loads. Here, we address the central question of which combinations are theoretically feasible for isotropic lattices.

C1. 2D lattices

Substituting equation (C1) into equations (2) through (4), we obtain:

$$\nu = \frac{A}{2B}\bar{\rho}^{(a-b)} - 1, \tag{C2}$$

$$= 1 - \frac{A}{2C}\bar{\rho}^{(a-c)}, \tag{C3}$$

$$= \frac{2C\bar{\rho}^{(c-b)}}{C\bar{\rho}^{(c-b)} + B} - 1, \tag{C4}$$

From (C2), it is clear that if $a < b$, then $\nu \to \infty$ as $\bar{\rho} \to 0$. Similarly, (C3) indicates that if $a < c$, then $\nu \to -\infty$ as $\bar{\rho} \to 0$. Therefore, for physically meaningful results, the following inequalities must hold:

$$a \geq b \quad \wedge \quad a \geq c. \tag{C5}$$

This leads to the conclusion that the following combinations of deformation modes are not possible (where S denotes "stretching-dominated" and B denotes "bending-dominated"): $a = 1$, $b = 1$, $c = 3$ (S, S, B); $a = 1$, $b = 3$, $c = 3$ (S, B, B); and $a = 1$, $b = 3$, $c = 1$ (S, B, S). In other words, if a lattice is stretching-dominated under uniaxial loading (i.e., $a = 1$), it must also be stretching-dominated both under shear and hydrostatic loadings, implying that $a = 1 \iff b = c = 1$.

In accordance with the inequalities in (C5), a potentially feasible scenario emerges with $a = 3$, $b = 1$, $c = 1$ (B,S,S). Substituting $a = 3$ and $b = 1$ into (C2) yields:

$$\nu = \frac{A}{2B}\bar{\rho}^2 - 1 \quad \Rightarrow \quad \nu \to -1 \quad \text{as} \quad \bar{\rho} \to 0. \tag{C6}$$

On the other hand, substituting $a = 3$ and $c = 1$ into (C3) produces:

$$\nu = 1 - \frac{A}{2C}\bar{\rho}^2 \quad \Rightarrow \quad \nu \to 1 \quad \text{as} \quad \bar{\rho} \to 0. \tag{C7}$$

The contradiction between the results from (C6) and (C7) indicates that the combination $a = 3$, $b = 1$, $c = 1$ (B, S, S) is also not feasible. FE analyses conducted in this paper have already established that the remaining four deformation combinations—(S, S, S), (B, B, B), (B, S, B), and (B, B, S)—are realizable and correspond to different lattice designs. The following sections will explore these feasible combinations in detail, along with their associated ranges of Poisson's ratio.

C1.1. a=b=c (S, S, S or B, B, B)

In cases where the lattice is either stretching- or bending-dominated under all loading conditions, Poisson's ratio simplifies to:

$$\nu = \frac{A}{2B} - 1, \tag{C8}$$

$$= 1 - \frac{A}{2C}, \tag{C9}$$

$$= \frac{2C}{C+B} - 1. \tag{C10}$$

Solving these equations yields the following relations:

$$A = \frac{4BC}{B+C}, \quad B = \frac{AC}{4C-A}, \quad C = \frac{AB}{4B-A}. \tag{C11}$$

The examination of equations (C8) to (C11) leads to the following conditions and their corresponding ranges for Poisson's ratio:

$$(2C < A < 4C \quad \wedge \quad A < 2B \quad \wedge \quad C < B) \quad \Rightarrow \quad -1 < \nu < 0 \tag{C12}$$

$$A = 2B = 2C \quad \Rightarrow \quad \nu = 0 \tag{C13}$$

$$(2B < A < 4B \quad \wedge \quad A < 2C \quad \wedge \quad B < C) \quad \Rightarrow \quad 0 < \nu < 1 \tag{C14}$$

$$(C \to 0 \iff A \to 4C) \quad \Rightarrow \quad (B \to B_{\mathrm{UB}} \quad \wedge \quad \nu \to -1) \tag{C15}$$

$$(B \to 0 \iff A \to 4B) \quad \Rightarrow \quad (C \to C_{\mathrm{UB}} \quad \wedge \quad \nu \to 1) \tag{C16}$$

C1.2. a=3, b=1, c=3 (B, S, B)

When the lattice is bending-dominated under uniaxial and hydrostatic loadings and stretching-dominated under shear, Poisson's ratio can be expressed as:

$$\nu = \frac{A}{2B}\bar{\rho}^2 - 1, \tag{C17}$$

$$= 1 - \frac{A}{2C}, \tag{C18}$$

$$= \frac{2C\bar{\rho}^2}{C\bar{\rho}^2 + B} - 1, \tag{C19}$$

leading to the following relations:

$$A = \frac{4BC}{B+C\bar{\rho}^2}, \quad B = \frac{AC\bar{\rho}^2}{4C-A}, \quad C = \frac{AB}{4B-A\bar{\rho}^2}. \tag{C20}$$

The effect of A, B, and C on Poisson's ratio can be expressed through the following conditions:

$$(2C < A < 4C \quad \wedge \quad A\bar{\rho}^2 < 2B \quad \wedge \quad C\bar{\rho}^2 < B) \quad \Rightarrow \quad -1 < \nu < 0 \tag{C21}$$

$$A\bar{\rho}^2 = 2B = 2C\bar{\rho}^2 \quad \Rightarrow \quad \nu = 0 \tag{C22}$$

$$(2B < A\bar{\rho}^2 < 4B \quad \wedge \quad A < 2C \quad \wedge \quad B < C\bar{\rho}^2) \quad \Rightarrow \quad 0 < \nu < 1 \tag{C23}$$

$$(C \to 0 \quad \vee \quad \bar{\rho} \to 0 \iff A \to 4C) \quad \Rightarrow \quad (B \to B_{\mathrm{UB}} \quad \wedge \quad \nu \to -1) \tag{C24}$$

$$(B \to 0 \iff A\bar{\rho}^2 \to 4B) \quad \Rightarrow \quad (C \to C_{\mathrm{UB}} \quad \wedge \quad \nu \to 1) \tag{C25}$$

C1.3. a=3, b=3, c=1 (B, B, S)

If the lattice is bending-dominated under uniaxial and shear loadings but stretching-dominated under hydrostatic loading, Poisson's ratio is given as follows:

$$\nu = \frac{A}{2B} - 1, \tag{C26}$$

$$= 1 - \frac{A}{2C}\bar{\rho}^2, \tag{C27}$$

$$= \frac{2C}{C + B\bar{\rho}^2} - 1. \tag{C28}$$

Accordingly, the relations among the parameters A, B, and C are given by:

$$A = \frac{4BC}{B\bar{\rho}^2 + C}, \quad B = \frac{AC}{4C - A\bar{\rho}^2}, \quad C = \frac{AB\bar{\rho}^2}{4B - A}. \tag{C29}$$

The conditions governing Poisson's ratio values in this scenario are:

$$(2C < A\bar{\rho}^2 < 4C \quad \wedge \quad A < 2B \quad \wedge \quad C < B\bar{\rho}^2) \quad \Rightarrow \quad -1 < \nu < 0 \tag{C30}$$

$$A\bar{\rho}^2 = 2B\bar{\rho}^2 = 2C \quad \Rightarrow \quad \nu = 0 \tag{C31}$$

$$(2B < A < 4B \quad \wedge \quad A\bar{\rho}^2 < 2C \quad \wedge \quad B\bar{\rho}^2 < C) \quad \Rightarrow \quad 0 < \nu < 1 \tag{C32}$$

$$(C \to 0 \iff A\bar{\rho}^2 \to 4C) \quad \Rightarrow \quad (B \to B_{\mathrm{UB}} \quad \wedge \quad \nu \to -1) \tag{C33}$$

$$(B \to 0 \quad \vee \quad \bar{\rho} \to 0 \iff A \to 4B) \quad \Rightarrow \quad (C \to C_{\mathrm{UB}} \quad \wedge \quad \nu \to 1) \tag{C34}$$

The parameters A, B, and C, along with the exponents a, b, and c, presented in Extended Data Tables 1 and 2 for various lattices, were obtained by fitting power functions to the finite element results. It is straightforward to demonstrate that, depending on the deformation mechanism of each lattice (as outlined in Table 1), the fitting coefficients can be substituted into the corresponding sets of equations and inequalities provided in sections C1.1, C1.2, or C1.3, resulting in perfect agreement.

C2. 3D lattices

For three-dimensional isotropic materials, the expressions for Poisson's ratio in terms of elastic moduli are given as:

$$\nu = \frac{A}{2B} - 1 = \frac{1}{2}\frac{E}{6K} = \frac{1}{2}\frac{3G}{2(G+3K)}. \tag{C35}$$

By plugging the effective elastic moduli given in (C1) into (C35), we arrive at the following representations for Poisson's ratio:

$$\nu = \frac{A}{2B}\bar{\rho}^{(a-b)} - 1, \tag{C36}$$

$$= \frac{1}{2} - \frac{A}{6C}\bar{\rho}^{(a-c)}, \tag{C37}$$

$$= \frac{1}{2} - \frac{3B\bar{\rho}^{(b-c)}}{2B\bar{\rho}^{(b-c)} + 6C}, \tag{C38}$$

As with the two-dimensional case, these equations yield physically meaningful values for Poisson's ratio only if the following conditions are met:

$$(a \geq b \quad \wedge \quad a \geq c) \quad \wedge \quad (b < a \quad \Longleftrightarrow \quad c = a). \tag{C39}$$

These constraints render certain deformation combinations infeasible: $a = 1$, $b = 1$, $c = 2$ (S, S, B); $a = 1$, $b = 2$, $c = 2$ (S, B, B); $a = 1$, $b = 2$, $c = 1$ (S, B, S); and $a = 2$, $b = 1$, $c = 1$ (B, S, S). Consequently, we are left with four viable combinations, analogous to those in the two-dimensional scenario.

Below we outline the relationships between Poisson's ratio ν and the parameters A, B, C, along with the conditions that must be fulfilled for ν to attain specific values in each of the possible deformation combinations.

C2.1. a=b=c (S, S, S or B, B, B)

$$\nu = \frac{A}{2B} - 1, \tag{C40}$$

$$= \frac{1}{2} - \frac{A}{6C}, \tag{C41}$$

$$= \frac{1}{2} - \frac{3B}{2B + 6C}, \tag{C42}$$

$$A = \frac{9BC}{B+3C}, \quad B = \frac{3AC}{9C-A}, \quad C = \frac{AB}{3(3B-A)}. \tag{C43}$$

$$(3C < A < 9C \quad \wedge \quad A < 2B \quad \wedge \quad 3C < 2B) \quad \Rightarrow \quad -1 < \nu < 0 \tag{C44}$$

$$A = 2B = 3C \quad \Rightarrow \quad \nu = 0 \tag{C45}$$

$$(2B < A < 3B \quad \wedge \quad A < 3C \quad \wedge \quad 2B < 3C) \quad \Rightarrow \quad 0 < \nu < 0.5 \tag{C46}$$

$$(C \to 0 \iff A \to 9C) \quad \Rightarrow \quad (B \to B_{\rm UB} \quad \wedge \quad \nu \to -1) \tag{C47}$$

$$(B \to 0 \iff A \to 3B) \quad \Rightarrow \quad (C \to C_{\rm UB} \quad \wedge \quad \nu \to 0.5) \tag{C48}$$

C2.2. a=2, b=1, c=2 (B, S, B)

$$\nu = \frac{A}{2B}\bar{\rho} - 1, \tag{C49}$$

$$= \frac{1}{2} - \frac{A}{6C}, \tag{C50}$$

$$= \frac{1}{2} - \frac{3B}{2B+6C\bar{\rho}}, \tag{C51}$$

$$A = \frac{9BC}{B+3C\bar{\rho}}, \quad B = \frac{3AC\bar{\rho}}{9C-A}, \quad C = \frac{AB}{3(3B-A\bar{\rho})}. \tag{C52}$$

$$(3C < A < 9C \quad \wedge \quad A\bar{\rho} < 2B \quad \wedge \quad 3C\bar{\rho} < 2B) \quad \Rightarrow \quad -1 < \nu < 0 \tag{C53}$$

$$A\bar{\rho} = 2B = 3C\bar{\rho} \quad \Rightarrow \quad \nu = 0 \tag{C54}$$

$$(2B < A\bar{\rho} < 3B \quad \wedge \quad A < 3C \quad \wedge \quad 2B < 3C\bar{\rho}) \quad \Rightarrow \quad 0 < \nu < 0.5 \tag{C55}$$

$$(C \to 0 \quad \vee \quad \bar{\rho} \to 0 \iff A \to 9C) \quad \Rightarrow \quad (B \to B_{\rm UB} \quad \wedge \quad \nu \to -1) \tag{C56}$$

$$(B \to 0 \iff A\bar{\rho} \to 3B) \quad \Rightarrow \quad (C \to C_{\rm UB} \quad \wedge \quad \nu \to 0.5) \tag{C57}$$

C2.3. a=2, b=2, c=1 (B, B, S)

$$\nu = \frac{A}{2B} - 1, \tag{C58}$$

$$= \frac{1}{2} - \frac{A}{6C}\bar{\rho}, \tag{C59}$$

$$= \frac{1}{2} - \frac{3B\bar{\rho}}{2B\bar{\rho}+6C}, \tag{C60}$$

$$A = \frac{9BC}{B\bar{\rho} + 3C}, \quad B = \frac{3AC}{9C - A\bar{\rho}}, \quad C = \frac{AB\bar{\rho}}{3(3B - A)}. \tag{C61}$$

$$(3C < A\bar{\rho} < 9C \quad \wedge \quad A < 2B \quad \wedge \quad 3C < 2B\bar{\rho}) \quad \Rightarrow \quad -1 < \nu < 0 \tag{C62}$$

$$A\bar{\rho} = 2B\bar{\rho} = 3C \quad \Rightarrow \quad \nu = 0 \tag{C63}$$

$$(2B < A < 3B \quad \wedge \quad A\bar{\rho} < 3C \quad \wedge \quad 2B\bar{\rho} < 3C) \quad \Rightarrow \quad 0 < \nu < 0.5 \tag{C64}$$

$$(C \to 0 \iff A\bar{\rho} \to 9C) \quad \Rightarrow \quad (B \to B_{\mathrm{UB}} \quad \wedge \quad \nu \to -1) \tag{C65}$$

$$(B \to 0 \quad \vee \quad \bar{\rho} \to 0 \iff A \to 3B) \quad \Rightarrow \quad (C \to C_{\mathrm{UB}} \quad \wedge \quad \nu \to 0.5) \tag{C66}$$

References

[1] Z. Hashin, S. Shtrikman, A variational approach to the theory of the elastic behaviour of multiphase materials, J. Mech. Phys. Solids 11 (2) (1963) 127–140.

[2] Z. Hashin, On elastic behaviour of fibre reinforced materials of arbitrary transverse phase geometry, J. Mech. Phys. Solids 13 (3) (1965) 119–134.

[3] R. Christensen, Mechanics of low density materials, J. Mech. Phys. Solids 34 (6) (1986) 563–578.

[4] G. Gurtner, M. Durand, Stiffest elastic networks, Proc. R. Soc. A. 470 (2164) (2014) 20130611.

[5] R. M. Christensen, Sufficient Symmetry Conditions for Isotropy of the Elastic Moduli Tensor, J. Appl. Mech. 54 (4) (1987) 772–777.

[6] C. Ayas, C. Tekoğlu, On the Sufficient Symmetry Conditions for Isotropy of Elastic Moduli, J. Appl. Mech. 85 (7) (2018) 074502.

[7] N. A. Fleck, V. S. Deshpande, M. F. Ashby, Micro-architectured materials: past, present and future, Proc. R. Soc. A. 466 (2010) 2495–2516.

[8] S. Hyun, S. Torquato, Effective elastic and transport properties of regular honeycombs for all densities, J. Mater. Res. 15 (9) (2000) 1985–1993.

[9] T. Tancogne-Dejean, N. Karathanasopoulos, D. Mohr, Stiffness and strength of hexachiral honeycomb-like metamaterials, J. Appl. Mech. 86 (11) (2019) 111010.

[10] S. Pellegrino, C. R. Calladine, Matrix analysis of statically and kinematically indeterminate frameworks, Int. J. Solids Struct. 22 (4) (1986) 409 – 428.

[11] S. Pellegrino, Structural computations with the singular value decomposition of the equilibrium matrix, Int. J. Solids Struct. 30 (21) (1993) 3025–3035.

[12] V. Deshpande, M. Ashby, N. Fleck, Foam topology bending versus stretching dominated architectures, Acta Mater. 49 (6) (2001) 1035–1040.

[13] S. Guest, J. Hutchinson, On the determinacy of repetitive structures, J. Mech. Phys. Solids 51 (3) (2003) 383–391.

[14] R. Hutchinson, N. Fleck, The structural performance of the periodic truss, J. Mech. Phys. Solids 54 (4) (2006) 756–782.

[15] O. A. Ickin, C. Tekoğlu, Structural Analysis of Periodic Trusses and Lattice Materials: States of Self-Stress, Mechanisms, and Mechanical Properties, J. Appl. Mech. (2024) 1–32.doi:10.1115/1.4066177.

[16] MATLAB, (R2023a), The MathWorks Inc., Natick, Massachusetts, 2023.

[17] T. Pronk, C. Ayas, C. Tekoğlu, A quest for 2D lattice materials for actuation, J. Mech. Phys. Solids 105 (2017) 199–216.

APPENDIX A: MATLAB CODE FOR THE STRUCTURAL ANALYSIS OF THE TWISTED KAGOME TRUSSES

```
%-------------------------------------------------------------%
% Clear all variables from the current workspace to free
% up system memory.
%-------------------------------------------------------------%
clear
%-------------------------------------------------------------%
% Variables used in the analysis:
%
% tht: The angle that defines the geometry of the infinite
%      periodic twisted Kagome truss
%      (see Supplementary Fig. 3a).
%
% rho: Relative density of the truss structure.
%
% E_s: Young's modulus of the material that makes up the
%      truss's cell walls.
%
% Lu: The unit bar length. For twisted Kagome Kagome truss,
%     all bars have the same length L = Lu
%     (see Supplementary Fig. 3a).
%
% A: The cross-sectional area of the bar elements.
%
% a, b, c, d, f, r, h, k, m: Direction cosines of the bar
% elements.
%
% UC_EL: The edge length of the unit cell (see Fig. XXX).
%
% E_ij (i, j in {1, 2}): Components of the externally
```

```
% imposed, macroscopically uniform strain field.
%
% d11, d12, d22: Deformations of the unit cell in response
% to the imposed macroscopic strains.
%
% Eij and nuij (i, j in {1, 2}) represent the truss's
% Young's modulus and Poisson's ratio in the i-j
% directions, respectively. G is the shear modulus
% of the truss.
%
% It is important to note that isotropic properties for the
% truss (E11 = E22 = 2G(1 + nu12) = 2G(1 + nu21)) are not
% assumed a priori. They emerge directly from the
% calculations.
%
% Also, the equation numbers referenced below correspond to
% the paper by Ickin, O. A., and Tekoglu, C.
% (August 7, 2024). "Structural Analysis of Periodic
% Trusses and Lattice Materials: States of Self-Stress,
% Mechanisms, and Mechanical Properties."ASME Journal of
% Applied Mechanics. doi: https://doi.org/10.1115/1.4066177
%-------------------------------------------------------%
syms tht E_11 E_22 E_12 rho E_s Lu A real
%
a=cos(tht);
b=cos(tht-pi/2);
c=cos(tht+pi/3);
d=cos(tht-pi/6);
f=cos(tht+2*pi/3);
r=cos(tht+pi/6);
h=cos(tht-2*pi/3);
```

```
k=cos(tht-pi/3);
m=cos(tht-pi);
%
L=Lu;
%
UC_EL=2*a*Lu;
%
d11=UC_EL*E_11/2;
d12=UC_EL*E_12/2;
d22=UC_EL*E_22/2;
%-------------------------------------------------------------%
% Steps 1 and 2 of the flowchart must be performed manually
% by the user.
%-------------------------------------------------------------%
% Step 3: Obtain and input the reduced kinematic
% matrix (BR).
%-------------------------------------------------------------%
BR=[0 0 a b -a -b; ...
    -c -d c d 0 0 ; ...
    -f -r 0 0 f r; ...
    h d 0 0 -h -d; ...
    k r -k -r 0 0; ...
    0 0 m b -m -b];
%-------------------------------------------------------------%
% Step 4: Compute the Z matrix as the null space of the
% transpose of the reduced kinematic matrix BR.
%-------------------------------------------------------------%
Z = null(transpose(BR));
%-------------------------------------------------------------%
% Step 5: Compute the Q matrix as the transpose of the null
% space of the transpose of Z.
```

```
%-------------------------------------------------------%
Q = transpose(null(transpose(Z)));
%-------------------------------------------------------%
% Step 6: Determine the P matrix.
% Since the bar length is uniform in the twisted Kagome
% truss, the P matrix is equal to the Q matrix
%-------------------------------------------------------%
P=Q;
%-------------------------------------------------------%
% Step 7: Solve Eq. (32) to express the bar elongation
% vector ({e}) in terms of the macroscopic strain
% components (E_ij). Perform the matrix concatenation as
% described in Eq. (32), where Left_C and Right_C
% correspond to the concatenated matrices on the left and
% right sides of the equation, respectively.
%-------------------------------------------------------%
Left_C=cat(1,P,Z(:,1).',Z(:,2).');
%
g(4,1)=(-h*d11+(sqrt(3)*h-d)*d12+sqrt(3)*d*d22);
g(5,1)=(k*d11+(sqrt(3)*k+r)*d12+sqrt(3)*r*d22);
g(6,1)=(-2*m*d11-2*b*d12);
%
Zero_Vector = zeros(4,1);
%
Right_C=cat(1,Zero_Vector,((Z.')*g));
%
e =linsolve(simplify(Left_C), simplify(Right_C));
%-------------------------------------------------------%
% Step 8: Calculate the components of the macroscopic
% stiffness tensor L_ijkl (S represents the area of the
% unit cell).
```

```
%-------------------------------------------------------%
S = sqrt(3)*UC_EL^2/2;
%
DeDeps11 = diff(e, E_11);
L1111 = simplify(dot(DeDeps11, DeDeps11)* ...
    E_s * A / Lu / S);
%
DeDeps22 = diff(e, E_22);
L2222 = simplify(dot(DeDeps22, DeDeps22)* ...
    E_s * A / Lu / S);
%
L1122 = simplify(dot(DeDeps11, DeDeps22)* ...
    E_s * A / Lu / S);
%
DeDeps12 = diff(e, E_12) / 2;
L1212 = simplify(dot(DeDeps12, DeDeps12)* ...
    E_s * A / Lu / S);
%-------------------------------------------------------%
% Step 9: Construct the stiffness matrix [L_Mat].
%-------------------------------------------------------%
L_Mat = [L1111 L1122 0;...
         L1122 L2222 0;...
         0 0 L1212];
%-------------------------------------------------------%
% Step 10: Calculate the mechanical properties.
% To express the mechanical properties in terms of the
% truss's relative density (rho), first normalize the
% moduli by the value of the relative density (rho_val),
% and then multiply the normalized values by rho.
%-------------------------------------------------------%
rho_val = simplify(sqrt(3)*A/(a^2*L));
```

```
%
nu12 = L1122/L2222;
nu21 = L1122/L1111;
E11 = L1111*(1-nu12*nu21)/rho_val*rho;
E22 = L2222*(1-nu12*nu21)/rho_val*rho;
G = L1212/rho_val*rho;
%
Modulus = ["E_11/E_s"; "E_22/E_s"; "nu_12"; "nu_21"; "G/E_s
   "];
Value = [E11/E_s; E22/E_s; nu12; nu21; G/E_s];
%-------------------------------------------------------------%
% Print the mechanical properties in a formatted table.
%-------------------------------------------------------------%
fprintf('<strong>Results for any tht value</strong>\n\n');
fprintf('<strong>Mechanical Properties:</strong>\n\n');
disp(table(Modulus, Value));
%-------------------------------------------------------------%
% Identify the macroscopic strain-producing mechanisms. For
% detailed information, refer to the paper: "A Quest for
% 2D Lattice Materials for Actuation," Journal of the
% Mechanics and Physics of Solids, 105 (2017), pp. 199-216.
%-------------------------------------------------------------%
BAUG=[0 0 a b -a -b 0 0 0; ...
    -c -d c d  0  0 0 0 0; ...
    -f -r 0 0  f  r 0 0 0; ...
    h  d  0 0 -h -d -h (sqrt(3)*h-d) sqrt(3)*d; ...
    k  r -k -r 0  0  k (sqrt(3)*k+r) sqrt(3)*r; ...
    0  0  m  b -m -b -2*m -2*b 0];
%-------------------------------------------------------------%
% Print null space of the augmented kinematic matrix.
%-------------------------------------------------------------%
```

```
fprintf(['<strong> Null space of the augmented ' ...
    'kinematic matrix:</strong>\n\n']);
NSAKM=null(BAUG);
disp(simplify(NSAKM));
%-------------------------------------------------------------%
% Print the vector that provides the relative ratios of the
% nodal displacements for the collapse mechanism under
% hydrostatic loading.
%-------------------------------------------------------------%
fprintf(['<strong>The relative ratios of the nodal ' ...
    'displacements for the</strong>\n']);
fprintf(['<strong>collapse mechanism under ' ...
    'hydrostatic loading</strong>\n\n']);
disp(simplify(NSAKM(:,3)));
```

APPENDIX B: MATLAB CODE FOR THE STRUCTURAL ANALYSIS OF THE HEXACHIRAL TRUSSES

```
%-------------------------------------------------------------%
% Clear all variables from the current workspace to free
% up system memory.
%-------------------------------------------------------------%
clear
%-------------------------------------------------------------%
% Variables used in the analysis:
%
% tht: The angle that defines the geometry of the infinite
%      periodic hexachiral truss
%      (see Supplementary Fig. 3b).
%
% a, b, c, d, f, r: Direction cosines of the bar elements.
%
% UC_EL = R: The edge length of the unit cell
%            (see Supplementary Fig. 3a).
%
% E_ij (i, j in {1, 2}): Components of the externally
% imposed, macroscopically uniform strain field.
%
% d11, d12, d22: Deformations of the unit cell in response
% to the imposed macroscopic strains.
%-------------------------------------------------------------%
syms tht R E_11 E_22 E_12 real
%
a=cos(pi/2-tht);
b=cos(tht);
c=cos(pi/6-tht);
d=cos(pi/3+tht);
```

```
f=cos(pi/6+tht);
r=cos(pi/3-tht);
%
UC_EL=R;
%
d11=UC_EL*E_11;
d12=UC_EL*E_12;
d22=UC_EL*E_22;
%-------------------------------------------------------------%
% Steps 1 and 2 of the flowchart must be performed manually
% by the user.
%-------------------------------------------------------------%
% Step 3: Obtain and input the reduced kinematic
% matrix (BR).
%-------------------------------------------------------------%
BR=[-a -b 0 0 0 0 a b 0 0 0 0;...
    0 0 -c -d 0 0 0 0 c d 0 0;...
    0 0 0 0 -f r 0 0 0 0 f -r;...
    -r -f r f 0 0 0 0 0 0 0 0;...
    0 0 -b a b -a 0 0 0 0 0 0;...
    0 0 0 0 -d c d -c 0 0 0 0;...
    0 0 0 0 0 0 r f -r -f 0 0;...
    0 0 0 0 0 0 0 0 b -a -b a;...
    -d c 0 0 0 0 0 0 0 0 d -c];
%-------------------------------------------------------------%
% Step 4: Compute the Z matrix as the null space of the
% transpose of the reduced kinematic matrix BR.
%-------------------------------------------------------------%
Z = null(transpose(BR))
%-------------------------------------------------------------%
% Z results in an empty set. This indicates that, in the
```

```
% low density limit, the hexachiral lattice exhibits
% bending-dominated behavior under all loading conditions,
% irrespective of the R/r ratio or the angle tht.
%-------------------------------------------------------%
if isempty(Z)
    fprintf(['<strong>Z results in an empty set. This ' ...
        'indicates that</strong>\n']);
    fprintf(['<strong>in the low density limit, the' ...
        ' hexachiral lattice</strong>\n']);
    fprintf(['<strong>exhibits bending-dominated' ...
        ' behavior under all loading</strong>\n']);
    fprintf(['<strong>conditions, irrespective of' ...
        ' the R/r ratio or the angle tht.</strong>\n\n']);
end
```

APPENDIX C: MATLAB CODE FOR THE STRUCTURAL ANALYSIS OF THE DOUBLE TRIANGULAR TRUSSES

```
%-------------------------------------------------------------%
% Clear all variables from the current workspace to free
% up system memory.
%-------------------------------------------------------------%
clear
%-------------------------------------------------------------%
% Variables used in the analysis:
%
% tht: The angle that defines the geometry of the infinite
%      periodic Double Triangular truss
%      (see Supplementary Fig. 3c). Note that the infinite
%      periodic Double Triangular truss exhibits
%      macroscopic strain-producing collapse mechanisms
%      only at tht = 60 degrees and tht = 145.6589 degrees.
%
% rho: Relative density of the truss structure.
%
% E_s: Young's modulus of the material that makes up the
%      truss's cell walls.
%
% Lu: The unit bar length. Specifically, bars 1 to 28, 32,
%     and 36 to 42 have a length L1 = Lu, while bars 29,
%     30, 31, 33, 34, and 35 have a length L2, defined as:
%     L2 = (sqrt(3) * d + sin(tht /2)) * Lu (see Fig. XXX).
%
% A: The cross-sectional area of the bar elements.
%
% a, b, c, d, f, r, h, k, m, n, p: Direction cosines of the
% bar elements.
```

```
%
% UC_EL: The edge length of the unit cell (see Fig. 1e).
%
% E_ij (i, j in {1, 2}): Components of the externally
% imposed, macroscopically uniform strain field.
%
% d11, d12, d22: Deformations of the unit cell in response
% to the imposed macroscopic strains.
%
% Eij and nuij (i, j in {1, 2}) represent the truss's
% Young's modulus and Poisson's ratio in the i-j
% directions, respectively. G is the shear modulus
% of the truss.
%
% It is important to note that isotropic properties for the
% truss (E11 = E22 = 2G(1 + nu12) = 2G(1 + nu21)) are not
% assumed a priori. They emerge directly from the
% calculations.
%
% Also, the equation numbers referenced below correspond to
% the paper by Ickin, O. A., and Tekoglu, C.
% (August 7, 2024). "Structural Analysis of Periodic
% Trusses and Lattice Materials: States of Self-Stress,
% Mechanisms, and Mechanical Properties."ASME Journal of
% Applied Mechanics. doi: https://doi.org/10.1115/1.4066177
%-------------------------------------------------------%
syms E_11 E_22 E_12 rho E_s Lu A
assume(Lu, "real");
tht=(30*pi/180);
% tht=(60*pi/180);
% tht=(145.658906273255289*pi/180);
```

```
%
a=cos(tht/2+pi/6);
b=cos(tht/2-pi/3);
c=cos(tht/2+pi/2);
d=cos(tht/2);
f=cos(tht/2-pi/6);
r=cos(tht/2-2*pi/3);
h=cos(tht/2-pi/2);
k=cos(tht/2-5*pi/6);
m=cos(tht/2+pi/3);
n=cos(pi/6);
p=cos(pi/3);
%
L1=Lu;
L2=(sqrt(3)*d+sin(tht/2))*Lu;
%
UC_EL=(4*f+2*h)*Lu;
%
d11=UC_EL*E_11;
d12=UC_EL*E_12;
d22=sqrt(3)/2*UC_EL*E_22;
%-------------------------------------------------------------%
% Steps 1 and 2 of the flowchart must be performed manually
% by the user.
%-------------------------------------------------------------%
% Step 3: Obtain and input the reduced kinematic
% matrix (BR).
%-------------------------------------------------------------%
BR = [-h -d h d 0 0 0 0 0 0 0 0 0 0 0 0 0 0 0 0 0 0 0 ...
    0 0 0 0 0 0 0 0 0 0 0 0 0 0 0;...
   -f -m 0 0 f m 0 0 0 0 0 0 0 0 0 0 0 0 0 0 0 0 0 ...
```

```
92      0 0 0 0 0 0 0 0 0 0 0 0 0 0;...
93      0 0 k b -k -b 0 0 0 0 0 0 0 0 0 0 0 0 0 0 0 0 0 0 ...
94      0 0 0 0 0 0 0 0 0 0 0 0 0 0;...
95      0 0 0 0 -f -r f r 0 0 0 0 0 0 0 0 0 0 0 0 0 0 0 0 ...
96      0 0 0 0 0 0 0 0 0 0 0 0 0 0;...
97      0 0 0 0 0 0 -k -b 0 0 k b 0 0 0 0 0 0 0 0 0 0 0 0 ...
98      0 0 0 0 0 0 0 0 0 0 0 0 0 0;...
99      0 0 -f -r 0 0 0 0 0 0 f r 0 0 0 0 0 0 0 0 0 0 0 0 ...
100     0 0 0 0 0 0 0 0 0 0 0 0 0 0;...
101     0 0 0 0 0 0 0 0 c d -c -d 0 0 0 0 0 0 0 0 0 0 0 0 ...
102     0 0 0 0 0 0 0 0 0 0 0 0 0 0;...
103     0 0 -a -b 0 0 0 0 a b 0 0 0 0 0 0 0 0 0 0 0 0 0 0 ...
104     0 0 0 0 0 0 0 0 0 0 0 0 0 0;...
105     0 0 0 0 0 0 -h -d 0 0 0 0 h d 0 0 0 0 0 0 0 0 0 0 ...
106     0 0 0 0 0 0 0 0 0 0 0 0 0 0;...
107     0 0 0 0 0 0 0 0 0 0 -f -m f m 0 0 0 0 0 0 0 0 0 0 ...
108     0 0 0 0 0 0 0 0 0 0 0 0 0 0;...
109     0 0 0 0 0 0 0 0 0 0 0 0 c d -c -d 0 0 0 0 0 0 0 0 ...
110     0 0 0 0 0 0 0 0 0 0 0 0 0 0;...
111     0 0 0 0 0 0 0 0 0 0 0 0 0 0 -a -b a b 0 0 0 0 0 0 ...
112     0 0 0 0 0 0 0 0 0 0 0 0 0 0;...
113     0 0 0 0 0 0 0 0 0 0 0 0 0 -f -r 0 0 f r 0 0 0 0 0 ...
114     0 0 0 0 0 0 0 0 0 0 0 0 0 0;...
115     0 0 0 0 0 0 0 0 0 0 0 0 0 0 -f -m 0 0 f m 0 0 0 0 ...
116     0 0 0 0 0 0 0 0 0 0 0 0 0 0;...
117     0 0 0 0 0 0 0 0 0 0 0 0 0 0 0 0 0 0 -a -b a b 0 0 ...
118     0 0 0 0 0 0 0 0 0 0 0 0 0 0;...
119     0 0 0 0 0 0 0 0 0 0 0 0 0 0 0 0 -f -m 0 0 f m 0 0 ...
120     0 0 0 0 0 0 0 0 0 0 0 0 0 0;...
121     0 0 0 0 0 0 0 0 0 0 0 0 0 0 0 0 0 0 0 0 -k -b k b ...
122     0 0 0 0 0 0 0 0 0 0 0 0 0 0;...
```

```
0 0 0 0 0 0 0 0 0 0 0 0 0 0 0 0 -h -d 0 0 0 0 h d ...
0 0 0 0 0 0 0 0 0 0 0 0 0 0 0;...
0 0 0 0 0 0 0 0 0 0 0 0 0 0 0 0 0 0 0 0 0 0 0 0 -f -r ...
f r 0 0 0 0 0 0 0 0 0 0 0 0 0;...
0 0 0 0 0 0 0 0 0 0 0 0 0 0 0 0 0 0 0 0 0 0 0 0 0 0 -c ...
-d c d 0 0 0 0 0 0 0 0 0 0;...
0 0 0 0 0 0 0 0 0 0 0 0 0 0 0 0 0 0 0 0 0 0 0 0 -a -b ...
0 0 a b 0 0 0 0 0 0 0 0 0 0;...
0 0 0 0 0 0 0 0 0 0 0 0 0 0 0 0 0 0 0 0 0 0 0 0 0 0 -h ...
-d 0 0 h d 0 0 0 0 0 0 0 0;...
0 0 0 0 0 0 0 0 0 0 0 0 0 0 0 0 0 0 0 0 0 0 0 0 0 0 0 ...
0 0 0 -c -d 0 0 c d 0 0 0 0;...
0 0 0 0 0 0 0 0 0 0 0 0 0 0 0 0 0 0 0 0 0 0 0 0 0 0 0 ...
0 -h -d 0 0 0 0 h d 0 0 0 0;...
0 0 0 0 0 0 0 0 0 0 0 0 0 0 0 0 0 0 0 0 0 0 0 0 0 0 0 ...
0 0 0 0 0 -f -m f m 0 0 0 0;...
0 0 0 0 0 0 0 0 0 0 0 0 0 0 0 0 0 0 0 0 0 0 0 0 0 0 0 ...
0 -k -b 0 0 k b 0 0 0 0 0 0;...
0 0 0 0 0 0 0 0 0 0 0 0 0 0 0 0 0 0 0 0 0 0 0 0 0 0 0 ...
0 0 0 -a -b 0 0 0 0 a b 0 0;...
0 0 0 0 0 0 0 0 0 0 0 0 0 0 0 0 0 0 0 0 0 0 0 0 0 0 0 ...
0 0 0 0 0 0 0 -f -r f r 0 0;...
0 0 0 0 0 0 0 0 0 0 -p -n 0 0 0 0 0 0 0 0 0 0 0 0 ...
0 0 0 0 0 0 0 0 0 0 0 0 0 p n;...
0 0 0 0 0 0 0 0 0 0 0 0 0 0 0 0 p -n 0 0 0 0 0 0 0 ...
0 0 0 0 0 0 0 0 0 0 0 0 -p n;...
0 0 0 0 0 0 0 0 0 0 0 0 0 0 0 0 0 0 0 0 0 0 0 0 0 0 0 ...
1 0 0 0 0 0 0 0 0 0 -1  0;...
0 0 0 0 0 0 0 0 -k -b 0 0 0 0 0 0 0 0 0 0 0 0 0 0 0 0 ...
0 0 0 k b 0 0 0 0 0 0 0 0;...
0 0 0 0 0 0 0 0 0 0 0 0 0 0 0 0 0 0 0 0 0 0 0 0 0 0 0 ...
```

```
    0 0 -1 0 0 0 0 0 0 0 1 0;...
    0 0 0 0 0 0 0 0 0 0 0 0 0 0 0 0 0 0 -p n 0 0 0 0 0 ...
    0 0 0 0 0 0 0 0 0 0 0 0 p -n;...
    0 0 0 0 p n 0 0 0 0 0 0 0 0 0 0 0 0 0 0 0 0 0 0 0 0 ...
    0 0 0 0 0 0 0 0 0 0 0 -p -n;...
    0 0 0 0 c d 0 0 0 0 0 0 0 0 0 0 0 0 0 0 0 0 0 0 0 0 ...
    0 0 0 0 -c -d 0 0 0 0 0 0;...
    0 0 0 0 0 0 a b 0 0 0 0 0 0 0 0 0 0 0 0 0 0 0 0 0 0 ...
    0 0 0 0 -a -b 0 0 0 0 0 0;...
    0 0 0 0 0 0 0 0 0 0 0 0 0 0 k b 0 0 0 0 0 0 0 0 0 0 ...
    0 0 0 0 0 0 0 0 -k -b 0 0;...
    0 0 0 0 0 0 0 0 0 0 0 0 0 0 0 0 0 0 h d 0 0 0 0 0 0 ...
    0 0 0 0 0 0 0 0 -h -d 0 0;...
    0 0 0 0 0 0 0 0 f m 0 0 0 0 0 0 0 0 0 0 0 0 0 0 -f ...
    -m 0 0 0 0 0 0 0 0 0 0 0 0;...
   -c -d 0 0 0 0 0 0 0 0 0 0 0 0 0 0 0 0 0 0 c d 0 0 0 ...
   0 0 0 0 0 0 0 0 0 0 0 0 0 0;...
    f r 0 0 0 0 0 0 0 0 0 0 0 0 0 0 0 0 -f -r 0 0 0 0 ...
    0 0 0 0 0 0 0 0 0 0 0 0 0 0];
%-------------------------------------------------------------%
% Step 4: Compute the Z matrix as the null space of the
% transpose of the reduced kinematic matrix BR.
%-------------------------------------------------------------%
Z = null(transpose(BR), 'r');
%-------------------------------------------------------------%
% Step 5: Compute the Q matrix as the transpose of the null
% space of the transpose of Z.
%-------------------------------------------------------------%
Q = transpose(null(transpose(Z)));
%-------------------------------------------------------------%
% Step 6: Determine the P matrix.
```

```
%-----------------------------------------------------------%
P = (Lu/L1)*Q;
for i=1: 36
    P(i,29)=(Lu/L2)*Q(i,29);
    P(i,30)=(Lu/L2)*Q(i,30);
    P(i,31)=(Lu/L2)*Q(i,31);
    P(i,33)=(Lu/L2)*Q(i,33);
    P(i,34)=(Lu/L2)*Q(i,34);
    P(i,35)=(Lu/L2)*Q(i,35);
end
%-----------------------------------------------------------%
% Step 7: Solve Eq. (32) to express the bar elongation
% vector ({e}) in terms of the macroscopic  strain
% components (E_ij). Perform the matrix concatenation as
% described in Eq. (32), where Left_C and Right_C
% correspond to the concatenated matrices on the left and
% right sides of the equation, respectively.
%-----------------------------------------------------------%
Left_C = cat(1, P, Z(:,1).', Z(:,2).', Z(:,3).', ...
    Z(:,4).', Z(:,5).', Z(:,6).');
%
g(32,1)=(-k*d11-b*d12);
g(33,1)=(d11);
g(34,1)=(0.5e0*p*d11-(sqrt(3.e0)/2.e0*p+0.5e0*n) ...
    *d12+n*d22);
g(35,1)=(0.5e0*p*d11+(sqrt(3.e0)/2.e0*p+0.5e0*n) ...
    *d12+n*d22);
g(36,1)=(0.5e0*c*d11+(sqrt(3.e0)/2.e0*c+0.5e0*d) ...
    *d12+d*d22);
g(37,1)=(0.5e0*a*d11+(sqrt(3.e0)/2.e0*a+0.5e0*b) ...
    *d12+b*d22);
```

```
g(38,1)=(0.5e0*k*d11+(sqrt(3.e0)/2.e0*k+0.5e0*b) ...
    *d12+b*d22);
g(39,1)=(0.5e0*h*d11+(sqrt(3.e0)/2.e0*h+0.5e0*d) ...
    *d12+d*d22);
g(40,1)=(f*d11+m*d12);
g(41,1)=(-c*d11-d*d12);
g(42,1)=(f*d11+r*d12);
%
Zero_Vector = zeros(36,1);
%
Right_C = cat(1, Zero_Vector, ((Z.')*g));
%
e = linsolve(vpa(Left_C), vpa(Right_C));
%-------------------------------------------------------------%
% Step 8: Calculate the components of the macroscopic
% stiffness tensor L_ijkl (S represents the area of
% the unit cell).
%-------------------------------------------------------------%
S = sqrt(3) * UC_EL^2 / 2;
%-------------------------------------------------------------%
% Note: The summation in Eq. (34) is performed using a dot
% product, as shown below. For bars 2, 4, 6, and 8, which
% have a length of (sqrt(2)/2) * Lu, we divide the
% elongation e_i by sqrt(sqrt(2)/2) for these bars
% (i in {2, 4, 6, 8}). This adjustment ensures that
% dividing the  dot product by Lu yields the correct length
% for each bar, as specified in Eq. (34).
%-------------------------------------------------------------%
e(29,:)=e(29,:)/(sqrt((sqrt(3)*d+sin(tht/2))));
e(30,:)=e(30,:)/(sqrt((sqrt(3)*d+sin(tht/2))));
e(31,:)=e(31,:)/(sqrt((sqrt(3)*d+sin(tht/2))));
```

```
e(33,:)=e(33,:)/(sqrt((sqrt(3)*d+sin(tht/2))));
e(34,:)=e(34,:)/(sqrt((sqrt(3)*d+sin(tht/2))));
e(35,:)=e(35,:)/(sqrt((sqrt(3)*d+sin(tht/2))));
%
DeDeps11 = diff(e, E_11);
L1111 = simplify(dot(DeDeps11, DeDeps11)* ...
    E_s * A / Lu / S);
%
DeDeps22 = diff(e, E_22);
L2222 = simplify(dot(DeDeps22, DeDeps22)* ...
    E_s * A / Lu / S);
%
L1122 = simplify(dot(DeDeps11, DeDeps22)* ...
    E_s * A / Lu / S);
%
DeDeps12 = diff(e, E_12) / 2;
L1212 = simplify(dot(DeDeps12, DeDeps12)* ...
    E_s * A / Lu / S);
%-------------------------------------------------------------%
% Step 9: Construct the stiffness matrix [L_Mat].
%-------------------------------------------------------------%
L_Mat = [L1111 L1122   0; ...
         L1122 L2222   0; ...
           0     0  L1212];
%-------------------------------------------------------------%
% Step 10: Calculate the mechanical properties.
% To express the mechanical properties in terms of the
% truss's relative density (rho), first normalize the
% moduli by the value of the relative density (rho_val),
% and then multiply the normalized values by rho.
%-------------------------------------------------------------%
```

```
rho_val =vpa((36.0+6.0*(sqrt(3)*d+sin(tht/2)))*Lu*A/S);
%
nu12 = L1122/L2222;
nu21 = L1122/L1111;
E11 = L1111*(1-nu12*nu21)/rho_val*rho;
E22 = L2222*(1-nu12*nu21)/rho_val*rho;
G = L1212/rho_val*rho;
%
Modulus = ["E_11/E_s"; "E_22/E_s"; "nu_12"; "nu_21"; ...
    "G/E_s"];
Value = [E11/E_s; E22/E_s; nu12; nu21; G/E_s];
%-------------------------------------------------------------%
% Print the mechanical properties in a formatted table.
%-------------------------------------------------------------%
fprintf(['<strong>Results for tht = %.10f' ...
    '</strong>\n\n'], tht*180/pi);
fprintf(['<strong>Mechanical Properties:' ...
    '</strong>\n\n']);
disp(table(Modulus, Value));
%-------------------------------------------------------------%
% Identify the macroscopic strain-producing mechanisms. For
% detailed information, refer to the paper: "A Quest for
% 2D Lattice Materials for Actuation," Journal of the
% Mechanics and Physics of Solids, 105 (2017), pp. 199-216.
%-------------------------------------------------------------%
BAUG=[-h -d h d 0 0 0 0 0 0 0 0 0 0 0 0 0 0 0 0 0 0 0 0 0 ...
    0 0 0 0 0 0 0 0 0 0 0 0 0 0 0 0 0 0 0 0 0;...
   -f -m 0 0 f m 0 0 0 0 0 0 0 0 0 0 0 0 0 0 0 0 0 0 0 ...
   0 0 0 0 0 0 0 0 0 0 0 0 0 0 0 0 0 0 0 0 0;...
    0 0 k b -k -b 0 0 0 0 0 0 0 0 0 0 0 0 0 0 0 0 0 0 0 ...
    0 0 0 0 0 0 0 0 0 0 0 0 0 0 0 0 0 0 0 0 0;...
```

```
0 0 0 0 -f -r f r 0 0 0 0 0 0 0 0 0 0 0 0 0 0 ...
0 0 0 0 0 0 0 0 0 0 0 0 0 0 0 0 0 0 0 0;...
0 0 0 0 0 0 -k -b 0 0 k b 0 0 0 0 0 0 0 0 0 0 ...
0 0 0 0 0 0 0 0 0 0 0 0 0 0 0 0 0 0 0 0;...
0 0 -f -r 0 0 0 0 0 0 f r 0 0 0 0 0 0 0 0 0 0 ...
0 0 0 0 0 0 0 0 0 0 0 0 0 0 0 0 0 0 0 0;...
0 0 0 0 0 0 0 0 c d -c -d 0 0 0 0 0 0 0 0 0 0 ...
0 0 0 0 0 0 0 0 0 0 0 0 0 0 0 0 0 0 0 0;...
0 0 -a -b 0 0 0 0 a b 0 0 0 0 0 0 0 0 0 0 0 ...
0 0 0 0 0 0 0 0 0 0 0 0 0 0 0 0 0 0 0 0;...
0 0 0 0 0 0 -h -d 0 0 0 0 h d 0 0 0 0 0 0 0 0 ...
0 0 0 0 0 0 0 0 0 0 0 0 0 0 0 0 0 0 0 0;...
0 0 0 0 0 0 0 0 0 0 -f -m f m 0 0 0 0 0 0 0 0 ...
0 0 0 0 0 0 0 0 0 0 0 0 0 0 0 0 0 0 0 0;...
0 0 0 0 0 0 0 0 0 0 0 0 c d -c -d 0 0 0 0 0 0 ...
0 0 0 0 0 0 0 0 0 0 0 0 0 0 0 0 0 0 0 0;...
0 0 0 0 0 0 0 0 0 0 0 0 0 0 -a -b a b 0 0 0 0 ...
0 0 0 0 0 0 0 0 0 0 0 0 0 0 0 0 0 0 0 0;...
0 0 0 0 0 0 0 0 0 0 0 0 0 0 -f -r 0 0 f r 0 0 0 0 ...
0 0 0 0 0 0 0 0 0 0 0 0 0 0 0 0 0 0 0 0;...
0 0 0 0 0 0 0 0 0 0 0 0 0 0 -f -m 0 0 f m 0 0 0 ...
0 0 0 0 0 0 0 0 0 0 0 0 0 0 0 0 0 0 0 0;...
0 0 0 0 0 0 0 0 0 0 0 0 0 0 0 0 0 0 -a -b a b 0 ...
0 0 0 0 0 0 0 0 0 0 0 0 0 0 0 0 0 0 0 0;...
0 0 0 0 0 0 0 0 0 0 0 0 0 0 0 0 0 0 -f -m 0 0 f m 0 ...
0 0 0 0 0 0 0 0 0 0 0 0 0 0 0 0 0 0 0 0;...
0 0 0 0 0 0 0 0 0 0 0 0 0 0 0 0 0 0 0 0 -k -b k ...
b 0 0 0 0 0 0 0 0 0 0 0 0 0 0 0 0 0 0 0 0;...
0 0 0 0 0 0 0 0 0 0 0 0 0 0 0 0 0 0 -h -d 0 0 0 0 h ...
d 0 0 0 0 0 0 0 0 0 0 0 0 0 0 0 0 0 0 0 0;...
0 0 0 0 0 0 0 0 0 0 0 0 0 0 0 0 0 0 0 0 0 0 -f -r ...
```

```
340     f r 0 0 0 0 0 0 0 0 0 0 0 0 0 0 0;...
341     0 0 0 0 0 0 0 0 0 0 0 0 0 0 0 0 0 0 0 0 0 0 0 0 0 0 0 ...
342     -c -d c d 0 0 0 0 0 0 0 0 0 0 0 0 0;...
343     0 0 0 0 0 0 0 0 0 0 0 0 0 0 0 0 0 0 0 0 0 0 0 0 0 -a -b ...
344     0 0 a b 0 0 0 0 0 0 0 0 0 0 0 0 0;...
345     0 0 0 0 0 0 0 0 0 0 0 0 0 0 0 0 0 0 0 0 0 0 0 0 0 0 0 ...
346     -h -d 0 0 h d 0 0 0 0 0 0 0 0 0 0;...
347     0 0 0 0 0 0 0 0 0 0 0 0 0 0 0 0 0 0 0 0 0 0 0 0 0 0 0 ...
348     0 0 0 0 -c -d 0 0 c d 0 0 0 0 0 0;...
349     0 0 0 0 0 0 0 0 0 0 0 0 0 0 0 0 0 0 0 0 0 0 0 0 0 0 0 ...
350     0 0 -h -d 0 0 0 0 h d 0 0 0 0 0 0;...
351     0 0 0 0 0 0 0 0 0 0 0 0 0 0 0 0 0 0 0 0 0 0 0 0 0 0 0 ...
352     0 0 0 0 0 0 -f -m f m 0 0 0 0 0 0;...
353     0 0 0 0 0 0 0 0 0 0 0 0 0 0 0 0 0 0 0 0 0 0 0 0 0 0 0 ...
354     0 0 -k -b 0 0 k b 0 0 0 0 0 0 0 0;...
355     0 0 0 0 0 0 0 0 0 0 0 0 0 0 0 0 0 0 0 0 0 0 0 0 0 0 0 ...
356     0 0 0 0 -a -b 0 0 0 0 a b 0 0 0 0;...
357     0 0 0 0 0 0 0 0 0 0 0 0 0 0 0 0 0 0 0 0 0 0 0 0 0 0 0 ...
358     0 0 0 0 0 0 0 0 -f -r f r 0 0 0 0;...
359     0 0 0 0 0 0 0 0 0 0 -p -n 0 0 0 0 0 0 0 0 0 0 0 0 0 ...
360     0 0 0 0 0 0 0 0 0 0 0 0 0 p n 0 0 0;...
361     0 0 0 0 0 0 0 0 0 0 0 0 0 0 0 0 0 p -n 0 0 0 0 0 0 ...
362     0 0 0 0 0 0 0 0 0 0 0 0 0 -p n 0 0 0;...
363     0 0 0 0 0 0 0 0 0 0 0 0 0 0 0 0 0 0 0 0 0 0 0 0 0 0 0 ...
364     0 0 1 0 0 0 0 0 0 0 0 0 -1  0 0 0 0;...
365     0 0 0 0 0 0 0 0 -k -b 0 0 0 0 0 0 0 0 0 0 0 0 0 0 0 ...
366     0 0 0 0 0 k b 0 0 0 0 0 0 0 0 -k -b 0;...
367     0 0 0 0 0 0 0 0 0 0 0 0 0 0 0 0 0 0 0 0 0 0 0 0 0 0 0 ...
368     0 0 0 0 -1 0 0 0 0 0 0 0 1 0 1 0 0;...
369     0 0 0 0 0 0 0 0 0 0 0 0 0 0 0 0 0 0 0 -p n 0 0 0 ...
370     0 0 0 0 0 0 0 0 0 0 0 0 0 p -n 0.5e0*p...
```

```
    -(sqrt(3.e0)/2.e0*p+0.5e0*n) n;...
    0 0 0 0 p n 0 0 0 0 0 0 0 0 0 0 0 0 0 0 0 0 0 ...
    0 0 0 0 0 0 0 0 0 0 0 0 -p -n 0.5e0*p...
    (sqrt(3.e0)/2.e0*p+0.5e0*n)  n;...
    0 0 0 0 c d 0 0 0 0 0 0 0 0 0 0 0 0 0 0 0 0 0 ...
    0 0 0 0 0 0 -c -d 0 0 0 0 0 0 0.5e0*c...
    (sqrt(3.e0)/2.e0*c+0.5e0*d)  d;...
    0 0 0 0 0 0 a b 0 0 0 0 0 0 0 0 0 0 0 0 0 0 0 ...
    0 0 0 0 0 0 -a -b 0 0 0 0 0 0 0.5e0*a...
    (sqrt(3.e0)/2.e0*a+0.5e0*b)  b;...
    0 0 0 0 0 0 0 0 0 0 0 0 0 0 k b 0 0 0 0 0 0 0 ...
    0 0 0 0 0 0 0 0 0 0 -k -b 0 0 0.5e0*k...
    (sqrt(3.e0)/2.e0*k+0.5e0*b)  b;...
    0 0 0 0 0 0 0 0 0 0 0 0 0 0 0 0 0 h d 0 0 0 0 ...
    0 0 0 0 0 0 0 0 0 0 -h -d 0 0 0.5e0*h...
    (sqrt(3.e0)/2.e0*h+0.5e0*d)  d;...
    0 0 0 0 0 0 0 0 f m 0 0 0 0 0 0 0 0 0 0 0 0 0 ...
    -f -m 0 0 0 0 0 0 0 0 0 0 0 f m 0;...
   -c -d 0 0 0 0 0 0 0 0 0 0 0 0 0 0 0 0 0 c d 0 0 ...
   0 0 0 0 0 0 0 0 0 0 0 0 0 -c -d 0;...
    f r 0 0 0 0 0 0 0 0 0 0 0 0 0 0 0 -f -r 0 0 0 ...
    0 0 0 0 0 0 0 0 0 0 0 0 0 0 0 f r 0];
%-------------------------------------------------------%
% Print null space of the augmented kinematic matrix.
%-------------------------------------------------------%
fprintf(['<strong> Null space of the augmented ' ...
    'kinematic matrix:</strong>\n\n']);
NSAKM=null(BAUG,'r');
disp(NSAKM);
%-------------------------------------------------------%
% Print the vector that provides the relative ratios of the
```

```
% nodal displacements for the collapse mechanism under
% hydrostatic loading at tht = 60 degrees.
%-------------------------------------------------------------%
if tht == (60*pi/180)
  fprintf(['<strong>The relative ratios of the nodal' ...
      ' displacements for the</strong>\n']);
  fprintf(['<strong>collapse mechanism under ' ...
      'hydrostatic loading:</strong>\n\n']);
  disp(NSAKM(:,3));
end
%-------------------------------------------------------------%
% Print the vector that provides the relative ratios of the
% nodal displacements for the collapse mechanism under
% pure shear loading at tht = 145.6589 degrees.
%-------------------------------------------------------------%
if tht == (145.658906273255289*pi/180)
  fprintf(['<strong>The relative ratios of the nodal' ...
      ' displacements for the</strong>\n']);
  fprintf(['<strong>collapse mechanism under ' ...
      'pure shear:</strong>\n\n']);
  disp(NSAKM(:,4));
end
```